1

D 3.2.1 HYDRODYNAMIC MODELS ANDFLUID DYNAMICS SIMULATIONS AND MODELING OF THE PROJECT AREAS

Annex to the Progress Report
December 2019
Version n.1

PROJECT AdSWiM

Work Package:	3. Harmonization of the knowledge, project areas modelling and mapping, activities planning
Activity:	3.2 Modelling and mapping of the project areas
Phase Leader:	OGS
Deliverable:	D3.2.1 by OGS

Version:	Final 1.0	Date:	20 December 2019
Type:	Model		
Availability:	Confidential		
Responsible Partner:	OGS		
Editor:	Stefano Querin [OGS]		
Contributors:	Mauro Celussi [OGS], Roko Andričević [UNIST-FGAG], Toni Kekez [UNIST-FGAG], Petra Šimundić [UNIST-FGAG]		

CONTENTS

PART 1: MODEL DESCRIPTION (NORTHERN ADRIATIC AREA)

The focus of the OGS activity is on the northern Adriatic sites (Lignano Sabbiadoro and San Giorgio di Nogaro discharge points).

The numerical model adopted is a customized version of the MITgcm, an open-source, state-of-the-art general circulation model developed at MIT. The setup of the AdSWiM simulations for the northern Adriatic features a 3D domain, with 27 vertical levels and a horizontal resolution of 1/128° (~700 m). The sewage discharge is simulated by a bottom flux (1 mmol/m2/s) of a generic eulerian tracer (proxy f**or** *Escherichia coli*) characterized by a first order decay law, function of temperature, salinity and solar radiation. The decay constants are obtained from the literature. Low salinity values (36) are also imposed to the bottom discharge cell, to simulate the buoyant plume of wastewater. In order to better plan the experimental activities, the numerical study simulates how the concentration of tracer varies in space and time during the year, under different environmental conditions.

PART 2: RESULTS (NORTHERN ADRIATIC AREA)

The model results (hydrodynamics) for the Lignano Sabbiadoro site are synthesized in Figure 1.
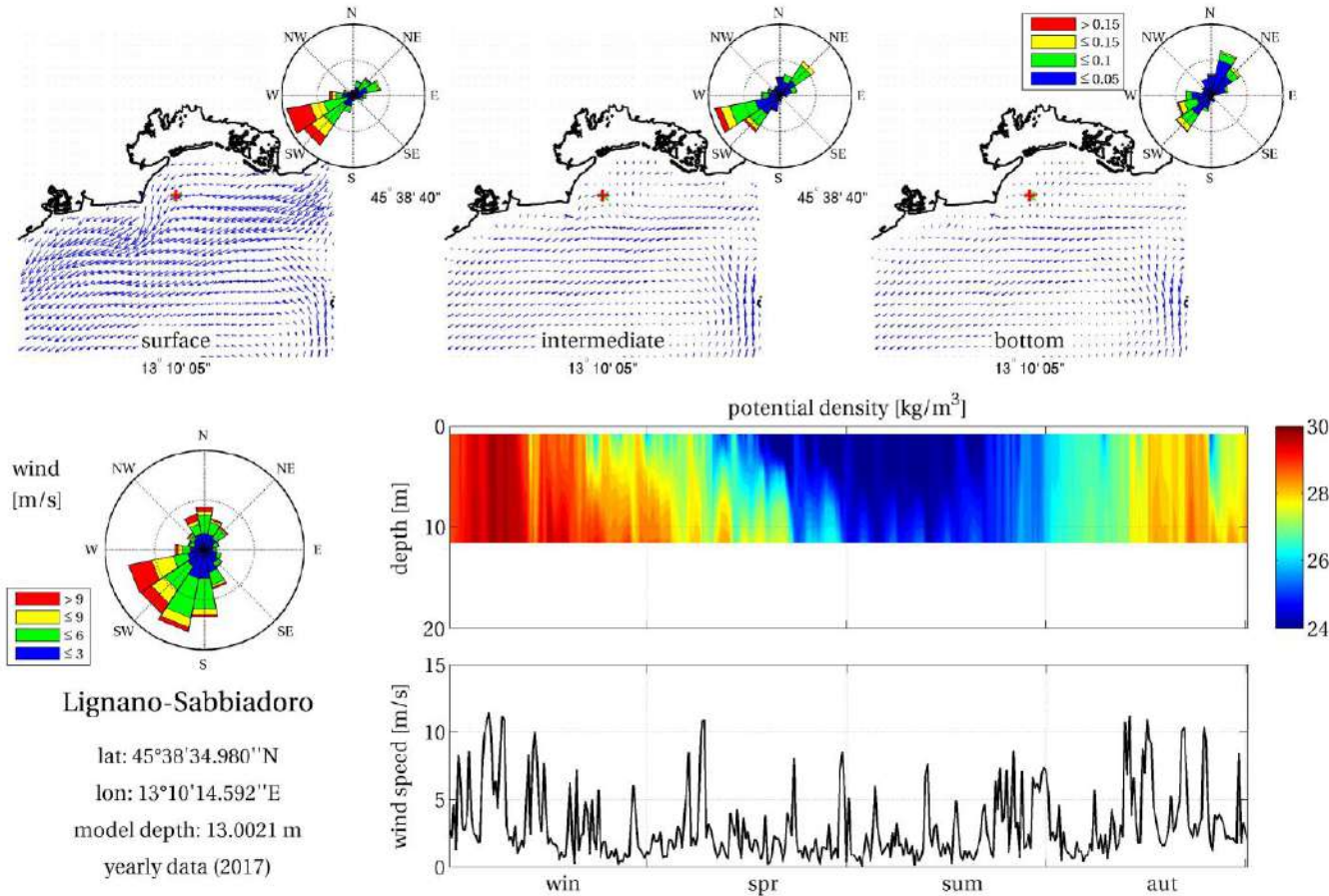
Figure 1: TOP: Average general circulation in the surroundings of the Lignano Sabbiadoro DP outfall with statistical distribution of the current field, at various levels (surface, average depth, bottom); BOTTOM LEFT: prevalent meteorological conditions (statistical distribution and time series of wind forcing); BOTTOM RIGHT: time series of the buoyancy properties (potential density) of the water column.

The 3 upper plots of Figure 1 show the spatial distribution of the average current vectors (blue arrows), in the surface, intermediate and bottom layer. The velocity arrows are plotted at every second grid point, for sake of readability. These plots provide information on the general circulation around the Lignano Sabbiadoro site. Moreover, the rosettes, on the upper-right corner of each vector plot, show the statistical distribution of the currents (direction and intensity) in the outfall point, for the same layer as for the general circulation maps (surface, intermediate, bottom). Current speed [m/s] is specified in the legend located in the upper right plot.

"Intermediate" and "bottom" refer to the model bathymetry for each site. In other words, "bottom" corresponds to the maximum model depth on each outfall site, "intermediate" corresponds to the level located halfway between the "surface" and the "bottom". The real outfall site is represented by the green "x" symbol, while the correspondent (i.e., the closest on the discretized domain) model grid point is indicated by the red "+" symbol.

The distribution of wind speed [m/s] and direction is reported in the central-left wind rose, with the corresponding legend.

For sake of simplicity, both wind and currents are plotted adopting the oceanographic convention: the current/wind spokes indicate the direction towards which the water/air is moving.

The two plots on the right-side show (upper plot) the time series of the vertical profiles (Hovmöller diagram) of potential density anomaly [kg/m3] and (lower plot) the wind speed [m/s].

The legend in the bottom-left corner of each figure reports the site name, the outfall coordinates, the depth of the model bathymetry in the corresponding grid point, and the time period considered (yearly analysis for 2017).

The same model, run for the San Giorgio di Nogaro site, is reported in Figure 2.

The results of the hydrodynamic models indicate a marked variability of current directions at the bottom layers, especially at the Lignano Sabbiadoro DP discharge point.
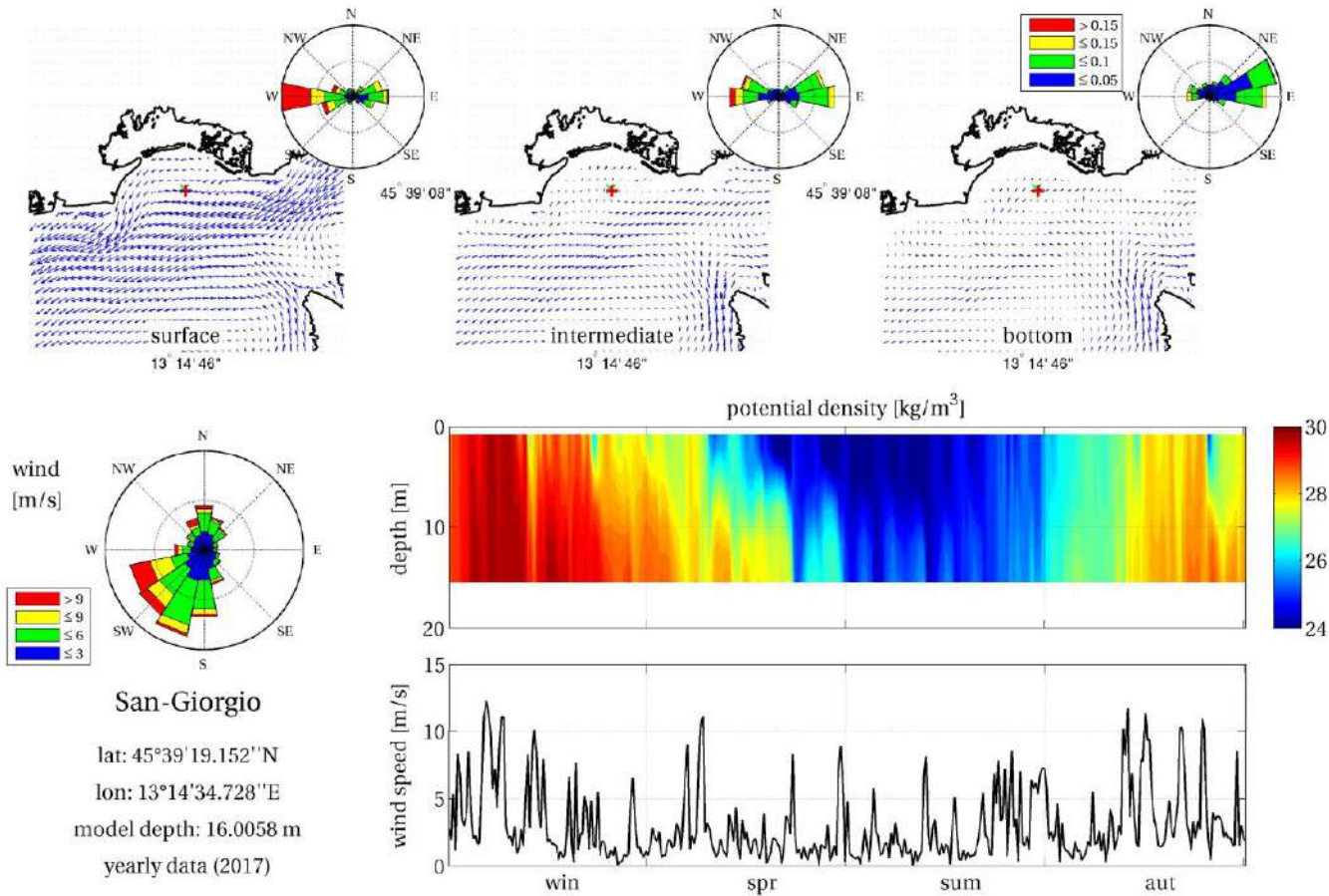
Figure 2: TOP: Average general circulation in the surroundings of the San Giorgio di Nogaro DP outfall with statistical distribution of the current field, at various levels (surface, average depth, bottom); BOTTOM LEFT: prevalent meteorological conditions (statistical distribution and time series of wind forcing); BOTTOM RIGHT: time series of the buoyancy properties (potential density) of the water column.

PART 3: MODEL DESCRIPTION AND RESULTS (ZADAR AND SPLIT AREAS)

The models for the Zadar and Split areas are described in the attached files "*Num.modeling Zadar site*" [Attachment 1] and "*Num.modeling Split sites*" [Attachment 2].

D 3.2.2 CROSS-BORDER MAPS WITHDPs AS HOT SPOTS OF RISK OF COASTAL POLLUTION

Annex to the Progress Report
December 2019
Version n.1

PROJECT AdSWiM

Work Package:	3. Harmonization of the knowledge, project areas modelling and mapping, activities planning
Activity:	3.2 Modelling and mapping of the project areas
Phase Leader:	OGS
Deliverable:	D3.2.2 by OGS

Version:	Final 1.0	Date:	20 December 2019
Type:	Model		
Availability:	Confidential		
Responsible Partner:	OGS		
Editor:	Stefano Querin [OGS]		
Contributors:	Mauro Celussi [OGS], Roko Andričević [UNIST-FGAG], Toni Kekez [UNIST-FGAG], Petra Šimundić [UNIST-FGAG]		

CONTENTS

PART 1: MODEL DESCRIPTION AND RESULTS (NORTHERN ADRIATIC AREA)

The focus of the OGS activity is on the northern Adriatic sites (Lignano Sabbiadoro and San Giorgio di Nogaro discharge points).

The numerical model adopted is a customized version of the MITgcm, an open-source, state-of-the-art general circulation model developed at MIT. The setup of the AdSWiM simulations for the northern Adriatic features a 3D domain, with 27 vertical levels and a horizontal resolution of 1/128° (~700 m). The sewage discharge is simulated by a bottom flux (1 mmol/m2/s) of a generic eulerian tracer (proxy for *Escherichia coli*) characterized by a first order decay law, function of temperature, salinity and solar radiation. The decay constants are obtained from the literature. Low salinity values (36) are also imposed to the bottom discharge cell, to simulate the buoyant plume of wastewater. In order to better plan the experimental activities, the numerical study simulates how the concentration of tracer varies in space and time during the year, under different environmental conditions.

The model results (pollutant dispersion) for the Lignano Sabbiadoro site are synthesized in Figure 1.
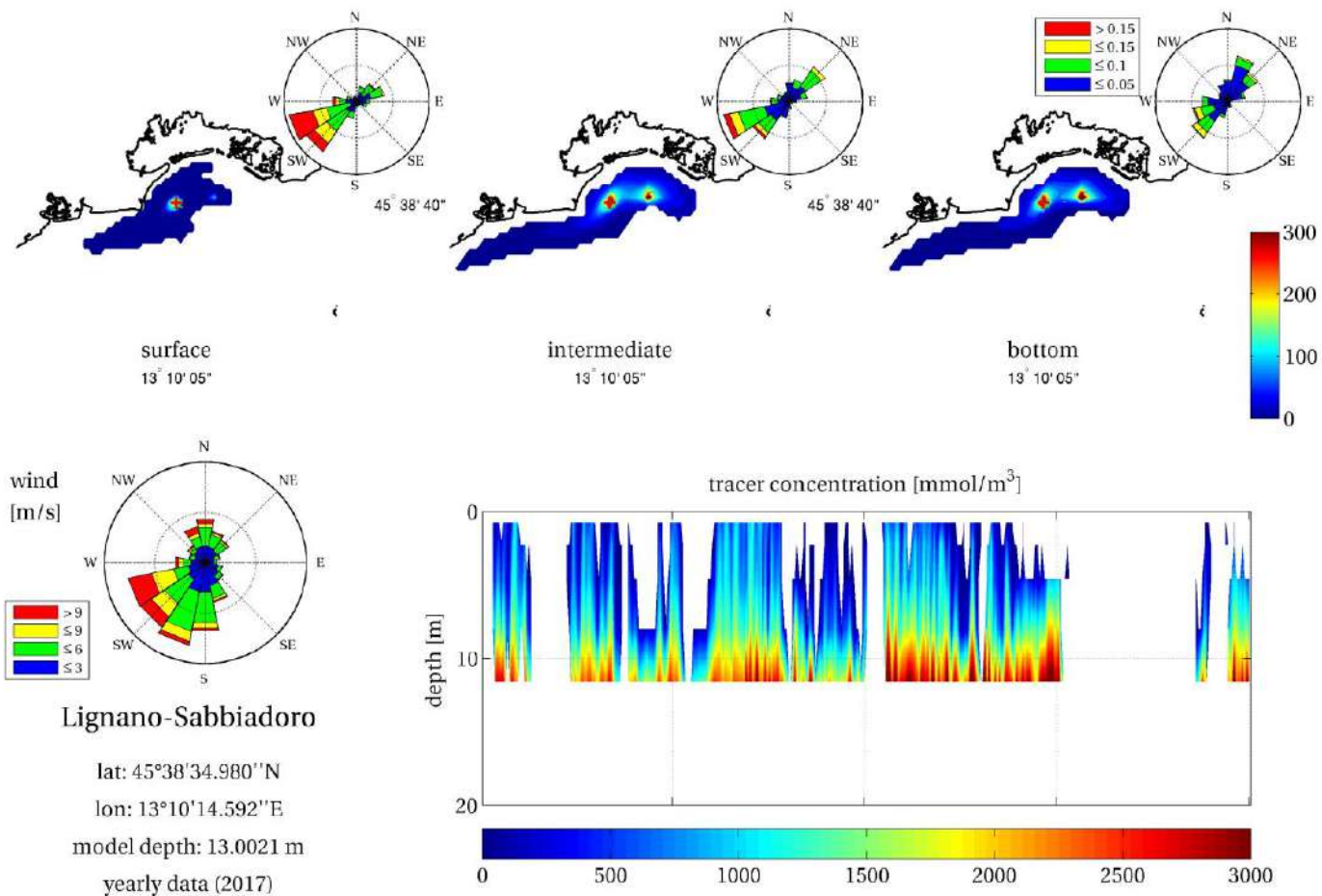
Figure 1: TOP: Average concentration of the tracer (mmol m^{-3}) in the surroundings of each outfall with statistical distribution of the current field, at various levels (surface, average depth, bottom); **BOTTOM LEFT:** prevalent meteorological conditions at the Lignano Sabbiadoro site (statistical distribution of wind speed); **BOTTOM RIGHT:** time series of the tracer concentration (proxy for *Escherichia coli*) in the water column.

The 3 upper plots show the spatial distribution of the average tracer concentration, in the surface, intermediate and bottom layer. These plots are useful to plan the monitoring activity and to locate the areas (on the sea floor and along the coast) potentially impacted by the discharged pollutants. Moreover, the rosettes, on the upper-right corner of each vector plot, show the statistical distribution of the currents (direction and intensity) in the outfall point, for the same layer as for the concentration maps (surface, intermediate, bottom). Current speed [m/s] is specified in the legend located in the upper right plot.

"Intermediate" and "bottom" refer to the model bathymetry for each site. In other words, "bottom" corresponds to the maximum model depth on each outfall site, "intermediate" corresponds to the level located halfway between the "surface" and the "bottom". The real outfall site is represented by the green "x" symbol, while the correspondent (i.e., the closest on the discretized domain) model grid point is indicated by the red "+" symbol.

The distribution of wind speed [m/s] and direction is reported in the central-left wind rose, with the corresponding legend.

The plot on the right side shows the time series of the vertical profiles (Hovmöller diagram) of tracer concentration [mmol m^{-3}]. Note that the color bars have different full-scale values (300 and 3000 mmol m^{-3} for yearly averages and vertical profiles, respectively).

The legend in the bottom-left corner of each figure reports the site name, the outfall coordinates, the depth of the model bathymetry in the corresponding grid point, and the time period considered (yearly analysis for 2017).

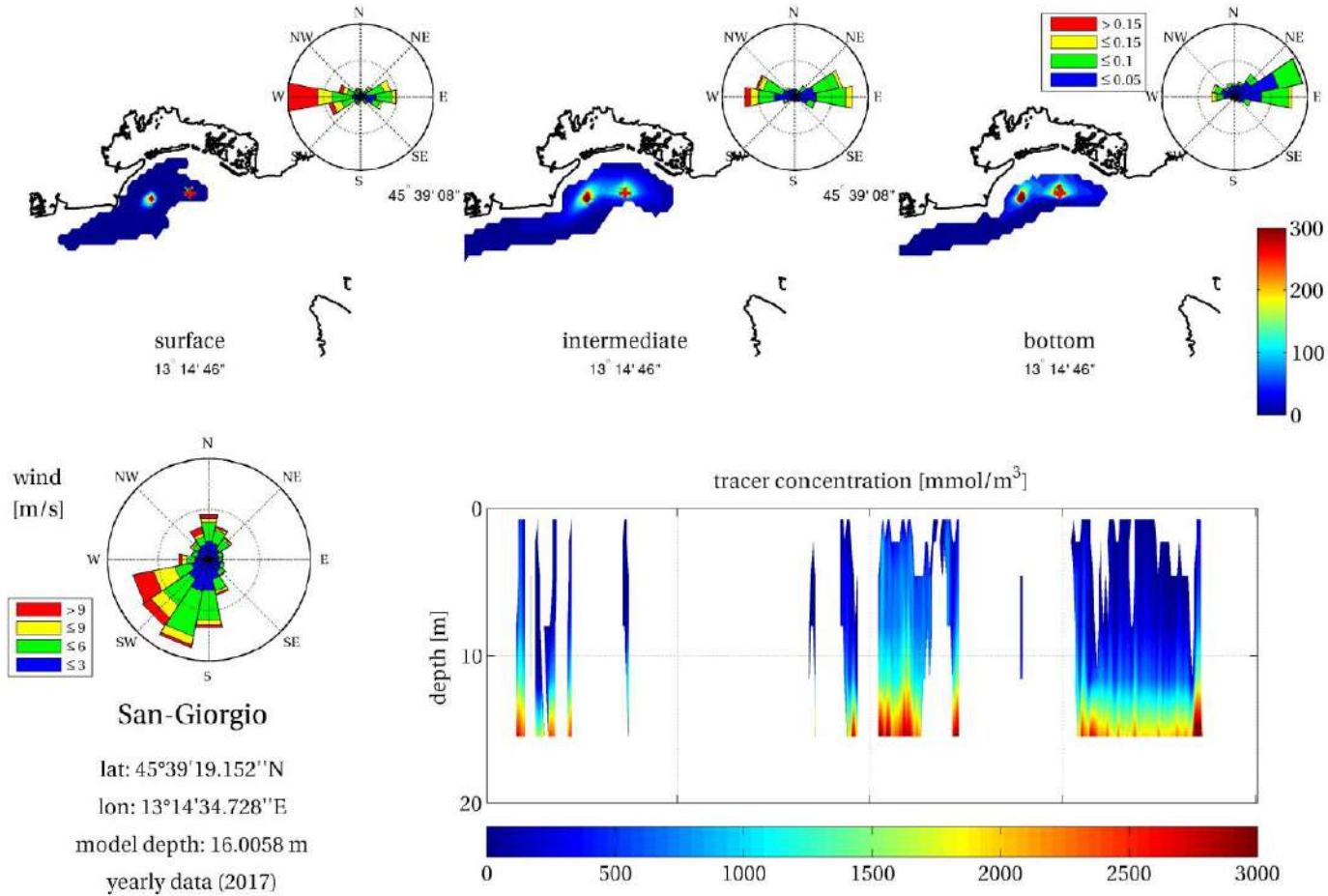The same model, run for the San Giorgio di Nogaro site, is reported in Figure 2.

Figure 2: TOP: Average concentration of the tracer (mmol m^{-3}) in the surroundings of each outfall with statistical distribution of the current field, at various levels (surface, average depth, bottom); **BOTTOM LEFT:** prevalent meteorological conditions at the San Giorgio di Nogaro site (statistical distribution of wind speed); **BOTTOM RIGHT:** time series of the tracer concentration (proxy for *Escherichia coli*) in the water column.

An animation of the model output is provided as attachment in the file "*AdSWiM_LS_SG_logos.mp4*". The movie shows the spreading of the tracer during the analyzed time period (2017). The concentrations, induced by a bottom flux of 1 mmol m^{-2} s^{-1}, are averaged every 6 hours (4 frames per day). The isosurfaces delimit the volumes with concentrations higher than 10 mmol m^{-3}. The low concentrations observed in summer are caused by the stronger intensity of the solar radiation, which leads to a higher decay ("mortality") of the particles.

The hydrodynamic model (D3.2.1) indicates a strong variability of bottom currents, thus preventing the definition of defined, fixed sampling points to monitor the DP discharge plume. Furthermore, the microbiological abundance data obtained during the 2019 sampling activities and historical data (D3.1.2) show a general absence of fecal indicators in the area, at least during the bathing season (from April to September). In the framework of the foreseen activities of 2020 (D3.3.1 and D3.3.2), the area will be further monitored for the presence of fecal indicators and emerging pathogenic bacteria.

PART 2: MODEL DESCRIPTION AND RESULTS (ZADAR AND SPLIT AREAS)

The models for the Zadar and Split areas are described in the attached files "*Num.modeling Zadar site*" and "*Num.modeling Split sites*".

1. INTRODUCTION

Croatian coast of the Adriatic Sea has complicated coastline and bathymetry with more than 1200 islands, innumerable channels, bays and inlets. Such complex geometry severely influences the coastal circulation mainly driven by meteorological and hydrological forcings. Although occasionally in some parts of the eastern coastal strip tidal currents and buoyancy-driven circulation can be important, in general these current components tend to be secondary in comparison with wind-induced motions.

Numerical models have been used a lot to interpret various aspects of the Adriatic Sea dynamics. One of the earliest numerical calculations was made in pre-computer era by Sterneck [1] and [2] and Defant [3] who integrated the frictionless hydrodynamic equations to study the Adriatic tides. More intensive use of numerical models in investigations of the Adriatic Sea dynamics coincided with introduction of computers in oceanography in the early 1970s. First computer model was made by Accerboni and Manca [4] in their study of the Adriatic tides. Early Adriatic computer models did not attempt to simulate the circulation but were simpler, storm-surge models with homogeneous density designed to calculate sea-surface elevation in response to wind events [5-9]. Particular attention was given to the simulation of bora storms and to prediction of flooding at Venice. Next important step in the numerical simulations in the Adriatic was made by Hendershott and Rizzoli [10]. They used a vertically integrated model to show the importance of topography upon the spreading of the deep water mass formed on the continental shelf of the northern Adriatic. In the late 1980s numerical modelling was concentrated on wind- driven circulation in the northern Adriatic [11-13] with particular attention paid to the response to bora events. Since then, there have been many regional and local model studies, utilizing *in situ* measurements and/or remote sensing techniques.

Contemporary modelling systems for the Adriatic Sea have been developed mostly within the framework of international project, e.g. *Project Adricosm*, *Mediterranean Forecasting system Pilot Project* etc. Basically, modern modelling system with realistic forcing consists of a hierarchy of more numerical models coupled among each other by nesting techniques, to downscale the larger scale flow field to highly resolved coastal scale fields. *In situ* and remote sensing data are used to evaluate modelling system performance, in particular a set of collected CTD measurements and satellite derived sea surface temperature measurements (SST), assessing a full three-dimensional picture of modelling systems quality.

For example, numerical modelling system launched within *Project Adricosm* (2001-2005) was set up in order to make an accurate forecast of short-term variability in the circulation of the Adriatic Sea, also giving some attention to the relevant processes in coastal areas. *In situ* measurements of individual parameters related to the atmosphere (meteorological parameters)

and the sea (physical, chemical, and biological parameters), and their temporal and spatial sampling dynamics were as follows: *in situ* VOS data (temperatures profiles with monthly sampling frequency), CTD data (temperature, salinity and oxygen collected bi-weekly), satellite data (SST at high resolution and surface chlorophyll - *SeaWiFS*), buoy data (temperature, salinity, oxygen, pH, light transmission and current velocity) and atmospheric forcing data (wind velocity, air temperature, dew point temperature and cloud cover).

Other recently launched operational sea circulation modelling systems for the Adriatic region also utilize *in situ* measurement as verification tool, with above mentioned data sets collected only in the open sea region. *In situ* measurements obtained in the eastern part of the Adriatic (channel region), e.g. permanent ADCP recording, were not included in model verification procedures. Numerical models of ecosystems can also be used as tools for forecasting and evaluating the influence of human activities, or for analyzing future changes to an ecosystem that may take place under the influence of external factors [14]. Biogeochemical models representing trophic and chemical interactions in the marine system have been discussed largely in the past 20 years [15-17], particularly focusing on a biomass-based description of the pelagic system. The biogeochemical rates of change are outlined starting from the parameterizations of the *European Regional Seas Ecosystem Model* (ERSEM) [18-19] which was the first comprehensive ecosystem model to include physiological considerations in the definition of the divergence of material fluxes. On the other hand several implementations of this model have shown the skill of this approach, both in coastal areas with large land-derived inputs but also in the oligotrophic Mediterranean regions [20-23]. The same approach has also been used in the context of climate studies, particularly to capture and analyze climate variability in the Adriatic Sea [24]. A direct descendant of ERSEM, the *Biogeochemical Flux Model* (BFM), has been developed in the framework of the EU project MFSTEP (*Mediterranean Forecasting System towards Environmental Predictions*) and applied to the whole Mediterranean basin and sub-regional seas.

Existing ecology modelling systems for the Adriatic Sea are validated and verified only on *in situ* measurement and remote sensed data collected in the open sea region, excluding the data sets obtained from monitoring campaigns undertaken within eastern part of the Adriatic (channel region).

During the implementation of *Phase I of The Adriatic Sea Monitoring Program* (hereafter *JP-07/09*), for the very first time, the current meter sites (25) and physical-biology-chemistry sites (45) were located at relatively small distances from the shore. *Phase I* of *JP-07/09* has already set up measurement necessary for the design of the models aimed to the analysis of some principal components of the sea water (coastal or marine water) quality in the eastern part of Adriatic Sea. For example, results of measurements within *JP-07/09* can be used for numerical modeling implementation (calibration) in the assessment of the impact of planned wastewater treatment facilities. The changes in the marine ecosystem are brought about by the discharge of effluents, in particular the treated municipal fecal wastewater. However, it should be pointed out that wastewater discharge is not the only form of pollution of the coastal parts of the Adriatic Sea.

In *JP-07/09* the following parameters were measured: sea temperature, salinity and density, sea currents, seawater transparency, dissolved oxygen, pH, nutrients (ammonium, nitrite, nitrate, orthophosphate, orthosilicate, total phosphorous, total nitrogen), biomass and phytoplankton composition (chlorophyll a), number of bacterial cells (direct microscopic counts), and fecal pollution indicators (fecal coliforms, fecal streptococci).

Physical processes in the middle Adriatic coastal area were studied within several national and international projects. The Zadar and Pašman channel area was investigated during early nineties due to the planned implementation of the public sewage system. Temperature, salinity and current measurements were made during two campaigns, the first one in June/July and the second one during August/September 2004, focused on the near coastal area. Although the main goal of Vilibić and Orlić [25] investigation were surface seiches and internal Kelvin waves in the Zadar and Pašman channel, they also calculated and discussed tidal, wind-induced and residual circulation. Tidal dynamics in the wider Zadar area is particularly interesting because of its close position to the Adriatic semidiurnal amphydromic point. The interesting feature of the residual dynamics was cyclonic and anticyclonic gyres, controlled by topography. Three-dimensional model [26] developed for the area off Zadar agreed with measurements and moreover indicated that vertically averaged currents at the basin mouth formed an anticyclonic gyre during a bora episode and a cyclonic gyre when sirocco wind blows.

Measurements in the open sea area off Zadar and Pašman channel were performed within international project 'East Adriatic Coastal Experiment' (EACE). Two maxima detected in the East Adriatic Current, the first one during winter and the second one during spring, were related to the water and heat air-sea fluxes, respectively [27]. Wind-induced currents were barotropic during winter and baroclinic during spring due to different stratification and stability conditions.

In this project the numerical analyses are focused on fecal pollution indicator transport (primarily E.Colli) in Zadar channel aquatory. Source of pollution is submarine outfall from water treatment facility Zadar – centar. The establishment of the model system of sea circulation and dynamics of E.Colli significantly relies on the results of monitoring within JP-07/09.

In the following second section of the report the basic characteristics of modelling system will be described. The third section presents the results of the modelling and their comparison with measurements, while final fourth section brings brief conclusions.

2. ESTABLISHING NUMERICAL MODELS OF SEA CIRCULATION AND E.COLLI TRANSPORT

Effluent transport phenomena in aquatic environment belong to the class of interdisciplinary problems (Fischer et al. 1979 [28]). Fluid mechanics traditional objective is focused on project solution optimization and analyzes of structure operability. On the other hand, geophysics fluid mechanics (meteorology, oceanography) is more oriented on the relevant processes comprehension and prediction on the broader temporal and spatial scales. Environmental fluid mechanics targets its primer major concern somewhere between those two extremes with the aim of assessing the potential environmental hazard impact and helping in decision making processes for the proposed project solutions (Cushman-Roisin et al. 2008 [29]).

Dominant forcing and their intensities in the mixing processes affecting the effluent plume on its pathway from the orifice of the diffuser to the arbitrary downstream profile are highly variable. Therefore, concept of separating of the far field and the near field zones with different dominant forcing is widely adopted (Fischer et al. 1979 [28]). In the case of the public sewage submarine outfall, near field domain in the vicinity of outfall diffuser, ranges from the inflow point up to the sea surface or neutral buoyancy layer where further effluent plume raising is interrupted and afterwards plume dynamics is mainly in the horizontal direction (Akar and Jirka 1994a [30], 1994b [31]). Therefore, integral solution of the problem is most commonly obtained through usage of combination of two structurally different numerical models. Plume propagation in the far field is modeled with 3D oceanographic numerical model using initial concentration fields calculated from the near field model (Akar and Jirka 1994a [30], 1994b [28], Wood et al. 1993 [32], Pun and Davidson 1999 [33]). Using described approach one can avoid high resolution numerical grid within the far field model required for resolving near field mixing process. That approach consists of two successive steps: a) temporal changes of vertical density distribution along the water column at the positions of the analyzed submarine outfall diffusers are obtained from 3D numerical model simulations; b) mixing processes in the near field are resolved using numerical model built up according Featherstone (1984) [34], with previously calculated vertical density profiles. More details about used near field numerical model are given in section 2.1.

2.1. *Near field transport model for E.Colli*

Near-field plume dynamics features were calculated with the use of the separate near-field numerical model, using information of the vertical density distribution previously calculated within 3D numerical model.

Near field effluent transport model is defined using set of differential equations for motion on steady control volume (Featherstone 1984 [34]). The core of the model consists of assuming initially effluent inflow through a circular nozzle opening and single buoyant jet or plume propagation without any interaction with other buoyant jets or plumes from adjacent nozzles.

Volume flux ϕ, mass flux ψ, specific momentum flux M, buoyancy flux B and specific buoyant force per unit length of a plume T are expressed with integral equations 1a-1e, where A represents a cross-sectional area of a plume orthogonal to the central trajectory, u represents velocity in the plume cross section, ρ density in the plume cross section, $\Delta\rho$ density deficit ($\Delta\rho = \rho_m - \rho$), ρ_m sea density and ρ_{m0} sea density at the position of diffuser nozzles.

$$\phi = \int_A u\,dA \qquad ; \qquad \psi = \int_A \rho u\,dA \qquad ; \qquad M = \int_A u^2\,dA \qquad \text{(1a,b,c)}$$

$$B = g \int_A \left(\frac{\Delta\rho}{\rho_{m0}}\right) \div u\,dA \qquad ; \qquad T = g \int_A \left(\frac{\Delta\rho}{\rho_{m0}}\right) \div dA \qquad \text{(1d,e)}$$

The core of the model is contained in the definition of the rate of change for ϕ, ψ, M and B fields along the central trajectory path s of the stationary plume. Neglecting the influence of ambient current on the overall plume dynamic, specific momentum rate of change becomes zero in the horizontal direction (eq. 2a). The change in the specific momentum in the vertical direction is caused by buoyancy (eq. 2b). Volume flux and mass flux change along the path s due to ambient fluid entrainment through the outer contour of the plume are defined with equation 3 (Turner, 1986 [35]). Henceforth specific momentum and volume flux follow:

$$\frac{d}{ds}(M\cos\theta) = 0 \; ; \quad \frac{d}{ds}(M\sin\theta) = T \qquad \text{(2a,b)}$$

$$\frac{d\phi}{ds} = E = 2\pi b\alpha u(s) \qquad \text{(3)}$$

where $u(s) = u(s,r=0)$ is velocity along the central trajectory of plume; b radial distance from central trajectory to the position where velocity assumes the value of $u(s,r=b) = u(s,r=0)/e$; $\alpha = 0.083$ entrainment constant (Featherstone, 1984); θ is angle of inclination of a tangent of a plume trajectory to the horizontal axis.

One assumes that velocity $u(s,r)$ and density deficit $\Delta\rho(s,r)$ follow Gauss's distribution in the plume cross section, using constant $\lambda = 1,16$ in case of scalar transport.

$$u(s, r) = u(s)e^{-r^2/b^2} \qquad ; \quad \Delta\rho(s, r) = \Delta\rho(s)e^{-r^2/(\lambda b^2)} \qquad \text{(4a,b)}$$

Integration of equation 1 (eq. 5) and definition of the proportionality between dB/ds and ϕ (eq. 6) along the streamline result in:

$$\phi = \pi u(s) b^2 \, (s) \qquad ; \qquad M = \frac{\pi u^2(s) b^2(s)}{2} \qquad\qquad (5a,b)$$

A1/7

$$B = \frac{\pi g \lambda^2 \Delta\rho\,(s)u(s)b^2(s)}{\rho_{m0}(1+\lambda^2)} \quad ; \quad T = \frac{\pi g \lambda^2 \Delta\rho(s)b^2(s)}{\rho_{m0}} \tag{5c,d}$$

$$\frac{dB}{ds} = \frac{g}{\rho_{m0}} \frac{d\rho_m}{ds} \phi \tag{6}$$

Substituting ϕ, M, B (eq. 5) in equations 2, 3, 6, and using some algebraic manipulations, one obtains the system of equations 7-11. Abbreviated character u and $\Delta\rho$ are used instead of $u(s)$ and $\Delta\rho(s)$ for the sake of simplicity:

$$\frac{du}{ds} = \frac{2g\lambda^2\Delta\rho}{\rho_{m0}u}\sin\theta - \frac{2\alpha u}{b} \tag{7}$$

$$\frac{db}{ds} = 2\alpha - \frac{g\lambda^2\Delta\rho b}{\rho_{m0}u^2}\sin\theta \tag{8}$$

$$\frac{d\theta}{ds} = \frac{2g\lambda^2\Delta\rho}{\rho_{m0}u^2}\cos\theta \tag{9}$$

$$\frac{d\Delta\rho}{ds} = \frac{(1+\lambda^2)}{\lambda^2}\frac{d\rho_m}{dz}\sin - \frac{2\alpha\Delta\rho}{b} \tag{10}$$

$$\frac{dx}{ds} = \cos\theta \quad ; \quad \frac{dz}{ds} = \sin\theta \tag{11a,b}$$

Dilution S is defined according Fan et al. (1966) [36],:

$$S(s) = \frac{4\lambda^2 u b^2}{(1+\lambda^2)u_0 d^2} \tag{12}$$

Integration of equation 7-11 begins where Gaussian profile (eq. 4) are fully developed e.g. at a distance of $s_0 = 6{,}2d$ (Featherstone 1984). Initial velocity u ($s = s_0 = 6{,}2d$) equals the mean exit velocity at diffuser nozzle $4\phi_0/(\pi d^2)$, while initial plume radius is obtained from conservation of momentum $b_0 = d/\sqrt{2}$.

The initial deflection of nozzle axis from horizontal plane θ_0 retains the same value up to the distance s_0 or θ ($s=s_0=6,2d$) $=\theta_0$. The value $\theta_0 = 0^0$ is used in the scope of numerical simulations, representing the case of horizontal nozzle set-up. Initial density difference at s_0 is assumed with

equality $\Delta\rho$ $(s = s_0 = 6,2d) = \Delta\rho_0 = [(\rho_{0m} - \rho_0)(1+\lambda^2)/(2\lambda^2)]$, initial coordinates of central plume trajectory with x $(s=s_0=6,2d) = x_0 = s_0 \cos\theta_0$ or $z(s = s_0 = 6,2d) = z_0 = s_0 \sin\theta_0$ and initial dilution with S $(s=s_0 = 6,2d) = S_0 = 2\lambda^2/(1+\lambda^2)$.

For solving the system of equations and in order to minimize local errors in the near field model Runge-Kutta 4. order method with variable spatial step was used. Model stops with integration when effluent plume reach the recipient surface or exceeds neutral buoyancy level.

The town of Zadar has developed public drainage system with respective water treatment facilities and submarine outfalls. The positions of water treatment facilities Zadar-centar and attached submarine outfall, including diffuser section, are indicated in Figure 1.
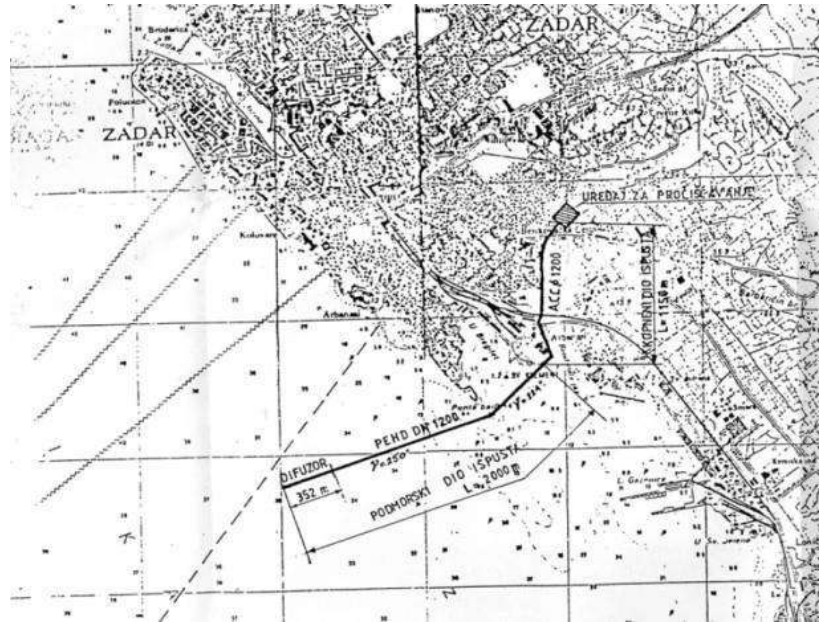
Figure 1 The positions of water treatment facilities Zadar-centar and attached submarine outfall

The land part of submarine outfall is 1150.3 m (diameter 1200 mm) and the submarine part is 2000 m (diameter 1200/1125 mm). The length of the diffuser is 352 m and ends at a depth of 34 m. Nozzles diameter is 15 cm. Submarine outfall works in non-stationary puls mode, what is also implemented in numerical model simulations. Figure 2 gives insight in recorded outfall discharge pulses during the period of highest consumption on one characteristic "summer" day. Initial concentration of EC for the near-field analyses (EC concentration in diffuser nozzle) is adoptet according to measured values on the enrtance section of submarine outfall, imidiatelly after water treatment facility (C_{EC} = $1.4*10^6$ cfu/100ml $\rightarrow$ 30.7.2019). Other possible sources of EC contamination in the analysed sea area were not taken into consideration.
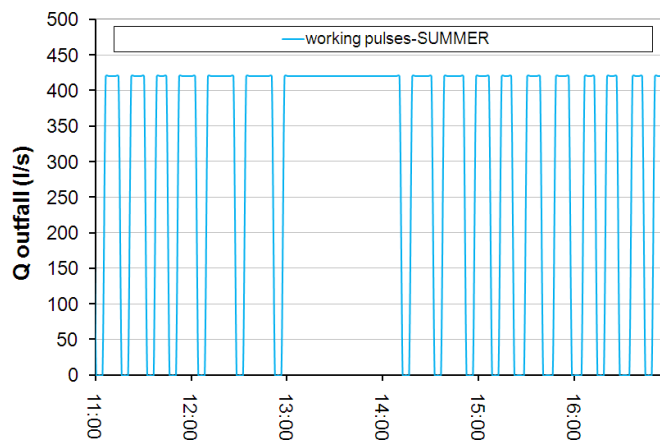
Figure 2 Zadar-centar submarine outfall discharge in nonstationary working mode (pulses) for sequence of characteristic "summer" day

2.2. *Sea circulation model (Mike 3 fm)*

One of the used models will be Mike 3fm with flexible mash approach. The modelling system has been developed for applications within oceanographic, coastal and estuarine environments. The Hydrodynamic Module is the basic computational component of the entire Mike 3fm modelling system providing the hydrodynamic basis for the Transport and ECO module.

The Hydrodynamic Module is based on the numerical solution of the three-dimensional incompressible Reynolds averaged Navier-Stokes equations subject to the assumptions of Boussinesq and of hydrostatic pressure. Thus, the model consists of continuity, momentum, temperature, salinity and density equations and is closed by a turbulent closure scheme.

$$\frac{\partial u}{\partial x} + \frac{\partial v}{\partial y} + \frac{\partial w}{\partial z} = S \tag{1}$$

$$\frac{\partial u}{\partial t} + \frac{\partial u^2}{\partial x} + \frac{\partial vu}{\partial y} + \frac{\partial wu}{\partial z} = fv - g\frac{\partial \eta}{\partial x} - \frac{1}{\rho_0}\frac{\partial p}{\partial x} - \frac{g}{\rho_0}\int_z^\eta \frac{\partial p}{\partial x}dz + F_u + \frac{\partial}{\partial z}\left(v_{tV}\frac{\partial u}{\partial z}\right) + u_s S \tag{2}$$

$$\frac{\partial v}{\partial t} + \frac{\partial v^2}{\partial y} + \frac{\partial uv}{\partial x} + \frac{\partial wv}{\partial z} = -fu - g\frac{\partial \eta}{\partial y} - \frac{1}{\rho_0}\frac{\partial p}{\partial y} - \frac{g}{\rho_0}\int_z^\eta \frac{\partial p}{\partial y}dz + F_v + \frac{\partial}{\partial z}\left(v_{tV}\frac{\partial v}{\partial z}\right) + v_s S \tag{3}$$

$$F_u = \frac{\partial}{\partial x}\left(2v_{tH}\frac{\partial u}{\partial x}\right) + \frac{\partial}{\partial y}\left(v_{tH}\left(\frac{\partial u}{\partial y} + \frac{\partial v}{\partial x}\right)\right) \tag{4}$$

$$F_v = \frac{\partial}{\partial x}\left(v_{tH}\left(\frac{\partial u}{\partial y} + \frac{\partial v}{\partial x}\right)\right) + \frac{\partial}{\partial y}\left(2v_{tH}\frac{\partial v}{\partial y}\right) \tag{5}$$

$$\rho = \rho(T, S) \tag{6}$$

$$\frac{\partial T}{\partial t} + u\frac{\partial uT}{\partial x} + \frac{\partial vT}{\partial y} + \frac{\partial wT}{\partial z} = F_T + \frac{\partial}{\partial z}\left(D_v\frac{\partial v}{\partial z}\right) + \hat{H} + T_s S \tag{7}$$

12

$$\frac{\partial S}{\partial t} + u\frac{\partial uS}{\partial x} + \frac{\partial vS}{\partial y} + \frac{\partial wS}{\partial z} = F_s + \frac{\partial}{\partial z}\left(D_v \frac{\partial S}{\partial z} \right) + S_S \tag{8}$$

$$(F_T, F_S) = \left[\frac{\partial}{\partial x}\left(D_h \frac{\partial}{\partial x} \right) + \frac{\partial}{\partial y}\left(D_h \frac{\partial}{\partial y} \right) \right](T, S) \tag{9}$$

$$\left\lfloor \quad \right\rfloor$$

$$D_h = \frac{\upsilon_{tH}}{\sigma_T} \quad ; D_v = \frac{\upsilon_{tV}}{\sigma_T} \tag{10}$$

$$v_{tV} = c_\mu \frac{k^2}{\varepsilon} \tag{11}$$

$$\frac{\partial k}{\partial t} + \frac{\partial uk}{\partial x} + \frac{\partial vk}{\partial y} + \frac{\partial wk}{\partial z} = F_k + \frac{\partial}{\partial z}\left(\frac{v_{tV}}{\sigma_k}\frac{\partial k}{\partial z}\right) + P + B - \varepsilon \tag{12}$$

$$\frac{\partial \varepsilon}{\partial t} + \frac{\partial u\varepsilon}{\partial x} + \frac{\partial v\varepsilon}{\partial y} + \frac{\partial w\varepsilon}{\partial z} = F_\varepsilon + \frac{\partial}{\partial z}\left(\frac{v_{tV}}{\sigma_\varepsilon}\frac{\partial \varepsilon}{\partial z}\right) + \frac{\varepsilon}{k}\left(c_{1\varepsilon}P + c_{3\varepsilon}B - c_{2\varepsilon}\varepsilon\right) \tag{13}$$

$$P = \frac{\tau_{xz}}{\rho_0\partial z}\frac{\partial u}{} + \frac{\tau_{yz}}{\rho_0\partial z}\frac{\partial v}{} \approx v_{tV}\left(\left(\frac{\partial u}{\partial z}\right)^2 + \left(\frac{\partial v}{\partial z}\right)^2\right) \tag{14}$$

$$B = -\frac{v_{tV}}{\sigma_t}N^2 \tag{15}$$

$$N^2 = -\frac{g}{\rho_0}\frac{\partial \rho}{\partial z} \tag{16}$$

$$\left(F_k, F_\varepsilon\right) = \left[\frac{\partial}{\partial x}\left(D_h\frac{\partial}{\partial x}\right) + \frac{\partial}{\partial y}\left(D_h\frac{\partial}{\partial y}\right)\right](k,\varepsilon) \; ; \; D_h = \frac{\upsilon_{tH}}{\sigma_k} \; ; \; D_h = \frac{\upsilon_{tH}}{\sigma_\varepsilon} \tag{17}$$

$$\upsilon_{tH} = c_s^2 I^2 \sqrt{2S_{ij}S_{ij}} \tag{18}$$

$$S_{ij} = \frac{1}{2}\left(\frac{\partial u_i}{\partial x_j} + \frac{\partial u_j}{\partial x_i}\right) \quad (i,j=1,2) \tag{19}$$

The free surface is taken into account using a sigma-coordinate transformation approach. The spatial discretization is performed using a cell-centered finite volume method. The spatial domain is discretized by subdivision of the continuum into non-overlapping element/cells. In the

15

horizontal plane an unstructured mesh is used while in the vertical domain a structured discretization is used. The elements can be prisms or bricks whose horizontal faces are triangles and quadrilateral elements, respectively.

Meshes are generated in the *MIKE Zero Mesh Generator*, which is a tool for the generation and handling of unstructured meshes, including the definition and editing of boundaries. Furthermore, the resolution in the geographical space is selected with respect to stability considerations.

The Hydrodynamic Module also calculates the resulting currents and distributions of salt, temperature, subject to a variety of forcing and boundary conditions. Baroclinic effect due to salt and temperature variations, and turbulence are considered as subordinated to the HD module. The density is assumed as a function of salinity and temperature, so the transport equations for

the temperature and/or salinity are solved simultaneously. Calculated temperature and salinity are feed-back to the hydrodynamic equations buoyancy forcing induced by density gradients.

Decomposition of the prognostic variables into a mean quantity and a turbulent fluctuation leads to additional stress terms in the governing equations to account for the non-resolved processes both in time and space. By the adoption of the eddy viscosity concept these effects are expressed through eddy viscosity and the gradient of the mean quantity, thus the effective shear stresses in the momentum equations contain the laminar stresses and the Reynolds stresses (turbulence).

The effects of submarine outfall are included in the simulation through as sources, taking into account the contribution to the continuity equation and the momentum equations.

The heat in the water can interact with the atmosphere through heat exchange. The heat exchange will be calculated on the basis of the four physical processes: the long wave radiation, the sensible heat flux (convection), the short wave radiation, the latent heat flux (evaporation). For the calculation of heat exchange influences the specification of air temperature, relative humidity and clearness coefficient as time variable series are utilized. Furthermore, for the latent heat flux constants in Dalton's and Sun constants in Angstrom's law are defined and together with the time displacement and the local standard meridian for the time zone incorporated in the calculation procedure. Heating by short wave radiation in the water column is also included. The short wave penetration which is dependent on the visibility is specified through light extinction coefficient.

The turbulence module is invoked from the specification of vertical eddy viscosity. The turbulence model is based on a standard k-ε model [37]. This model uses transport equations for the turbulent kinetic energy - k and its dissipation - ε.

3D numerical model of sea circulation, as a basis for further analyses of E.Colli transport in far-field, is established with spatial domain that covers the area of Zadar channel (Fig. 3). The simulations are carried out for the period from 4 July 2008 to 22 August 2008.

The numerical model domain uses a calculation mesh with a variable spatial step from 30m to 150m. Near the respective open boundaries (Fig. 3) there is at least one monitoring station from which it is possible to collect data on boundary conditions (Fig. 4).

Numerical integration of the sea circulation model started on 4.7.2008 by initiation with the sea temperature and salinity fields at standard oceanographic depths from the oceanographic database of Dartmouth College (Fig. 5, Dartmouth Adriatic Data Base – DADB [38]).

At the open boundaries the model was forced with hourly dynamic of sea levels [39], along with the sea temperature (T) and salinity (S) fields according to the measured vertical distributions of T and S at the nearest oceanographic station used within the implementation of this monitoring program JP-07/09 (Fig. 6).

The fields of wind, air temperature, humidity and cloudiness were defined based on the results of the atmospheric numerical model Aladin-HR [40-44]. The used wind fields from the model Aladin-HR have a forecasting character (+12h) and spatial and temporal resolution of 8km and 3h, respectively (Figure 7).
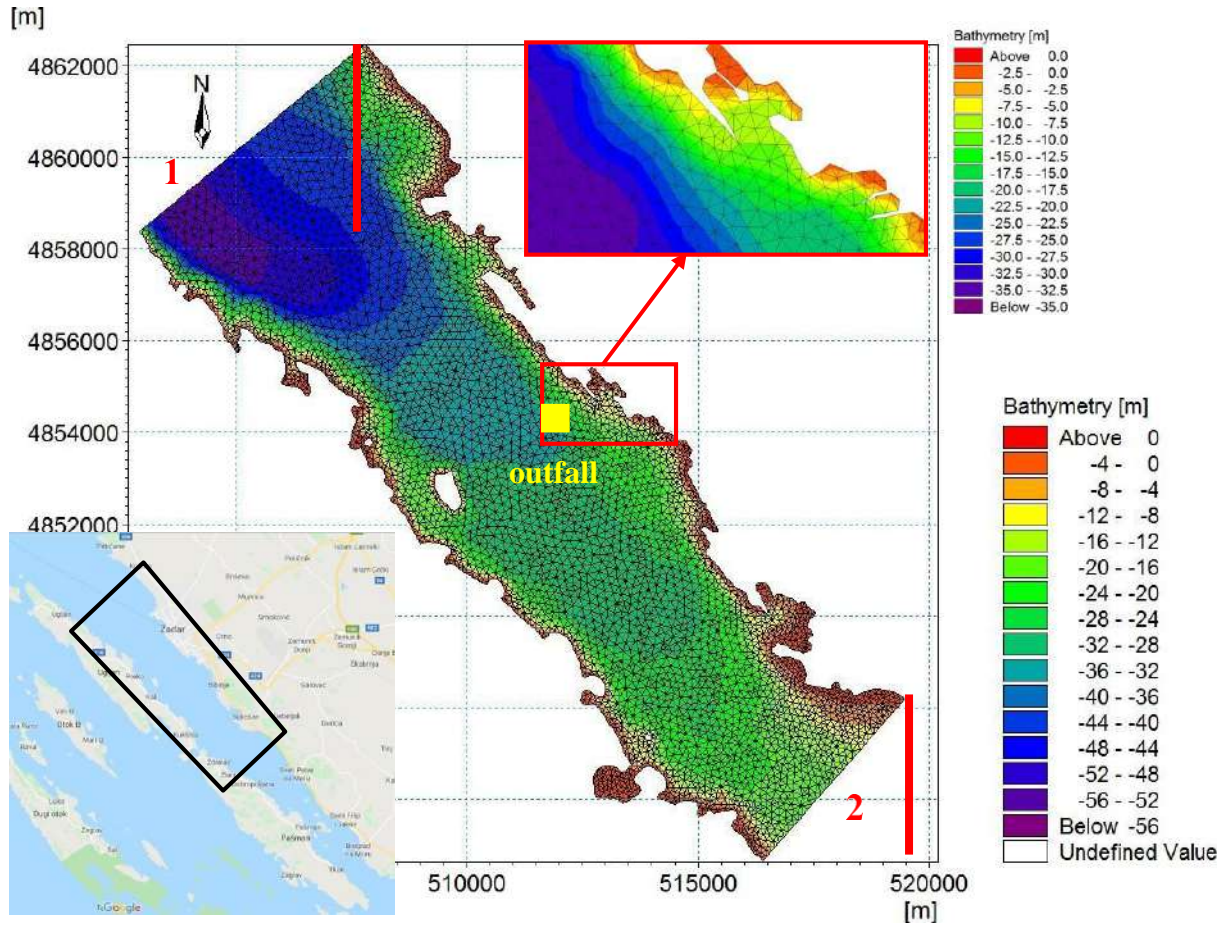

Figure 3 Numerical model spatial domain and respective discretization with finite volumes on bathymetry background (Mike 3fm, open boundaries are indicated with numbers 1 and 2)

Figure 4 Locations of oceanographic stations during the implementation of the *Adriatic Sea Monitoring Program* (*JP-07/09*)
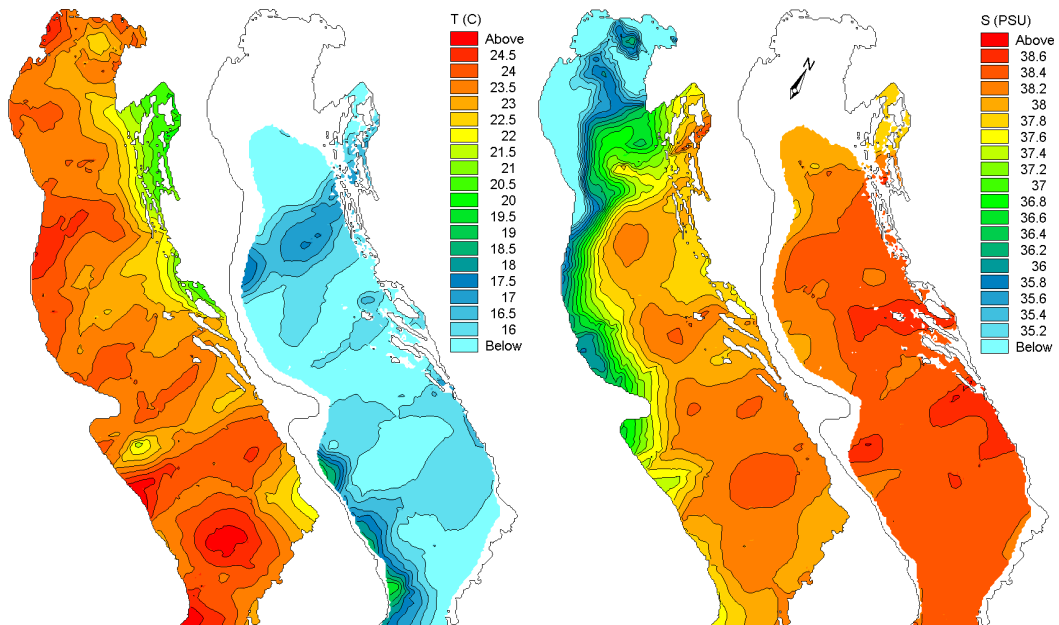
Figure 5 Sea temperature and salinity fields in the surface layer and at a depth of 50m for the area of the entire Adriatic (summer period - 1 July 2008 [38])
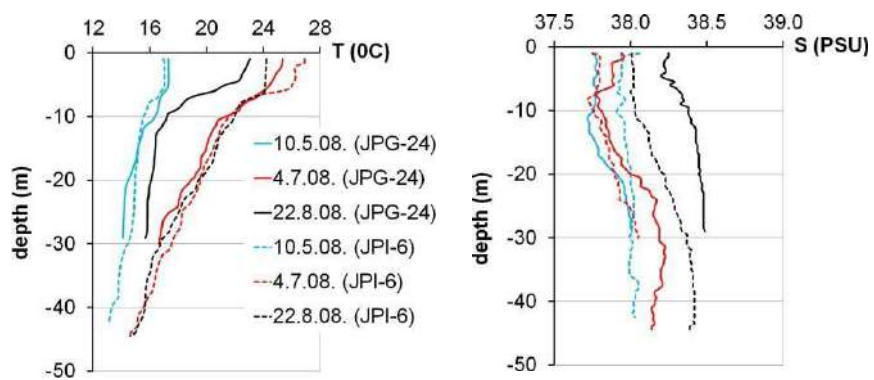
Figure 6 Measured vertical distributions of T and S at the oceanographic stations JPG-24 and JPI-6 (see Fig. 4)
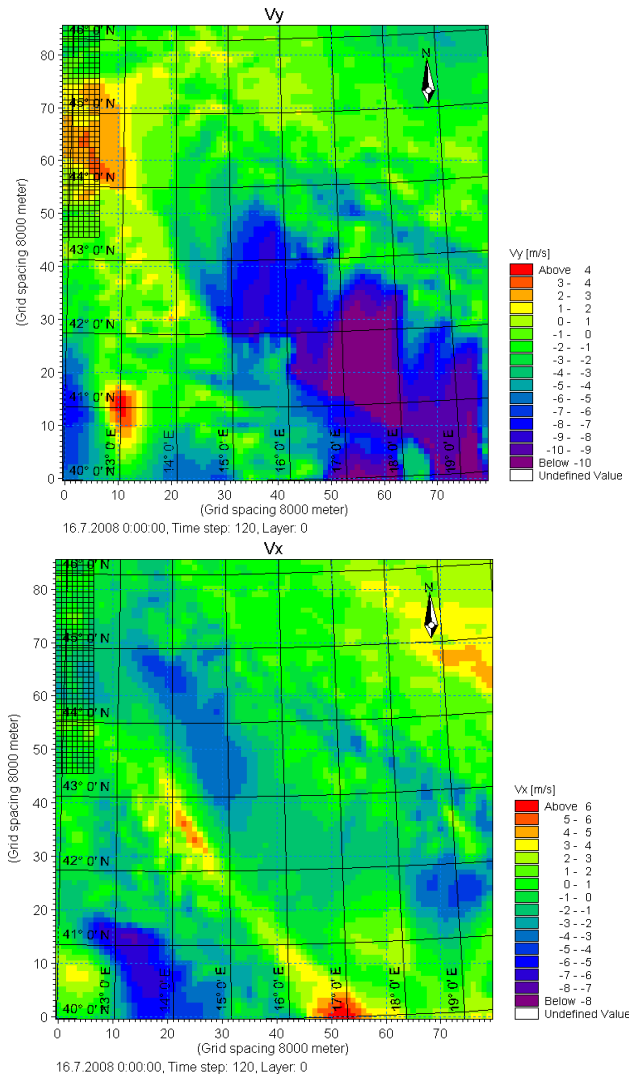
Figure 7 Example of resultant fields from the atmospheric model Aladin-HR for the term 16/7/08 0:00 (left - v_x wind velocity component at 10m from the sea surface; right - v_y velocity component)

2.3. Far field transport model for E.Colli

The user designs mathematical form to interpret time dynamics of E.Colli concentration within ecological processes with all interactions and connections among variables in a process. Defined process variables are spatially transferred through the connection with a convective dispersive module or hydrodynamic module.

Every designed mathematical form uses process variables, constants, forcing parameters and auxiliary variables, all incorporated through process equations. Process variables give the best insight into a state of a particular eco system and are chosen to predict system behavior by monitoring of their dynamics. Constants are used as arguments in mathematical formulas describing systems, and are time invariant but can be spatial variables. Forcing parameters are used as arguments in mathematical formulas describing systems, and can be both spatial and time variables. These parameters represent variables by which external influences on eco system e.g. temperature, solar radiation, wind etc., are involved. Auxiliary variables are also arguments in mathematical (numerical) formulas describing systems, and are sometimes used for direct

result specification only. Processes give a mathematical description of the process variable transformation, meaning that processes are used as arguments in differential equations which are solved by ecological module for determination of the state of a process variable.

An ordinary differential equation is specified for each state variable. The ordinary differential equation summaries the processes evolved for the specific state variable. If a process affects more than one state variable, or the state variables affect each other, the differential equations are coupled with each other. The state variables are coupled linearly or non-linearly to each other through the source/sink terms. Defined numerical equations are solved using the built-in solver that makes an explicit time-integration of the transport equations when calculating the concentrations to the next time step. An approximate solution is obtained by treating the advection-dispersion term as constant in each time step. Defined coupled set of ordinary differential equations are solved by integrating the rate of change due to both the defined processes themselves and the advection-dispersion processes.

In E.Coli transport analisys the numeric formulation which treats E.Colli concentration as process variables of the ecosystem is used. The differential equation of the rate of E.Colli concentration change is created, using appropriate variables, constants, forcing parameters and auxiliary variables. Decay of E.Colli is described by the linear model of decay (Lee, 2011 [45]):

$$\frac{dC}{dt} = -[K * STI * C] \qquad ; \qquad K = \frac{Ln(10)}{T_{90}} \tag{13}$$

where: C E.Colli concentration [1/100ml], K decay coefficient at 20°C in fresh water in darkness (1,08 1/dan, De Brauwere et al. [46]), STI correction decay coefficient for temperature, salinity, and light,

$$STI = \theta_T{}^{T-20} * \theta_S{}^S * \theta_I{}^{I(t,z)} \tag{14}$$

where: θ_T temperature correction coefficient for decay coefficient at temperatures different from 20 C^0 (1,09 – Jorgensen, 2001 [47]), T sea temperature, θ_S correction coefficient for salinity different from clean water (1,006 - Jorgensen, 2001), S salinity, θ_I correction coefficient for the influence of light (7,4 - Jorgensen, 2001 [47]).

Vertical light distribution is defined by exponential law as a function of depth according to the Lambert-Beer law:

$$I(t,z) = f(t) \, I_0 \, e^{-kz} \tag{15}$$

where: I_0 light intensity at the surface at noon (k =2,3/secchi depth).

3. COMBINING MEASUREMENTS AND MODEL

Model simulations for sea circulation are performed for the period 4 July 2008 - 22 August 2008, since monitoring was conducted in that period on current meter and CTD measuring stations, which resulted in extensive set of data suitable for the verification of model results of thermohaline properties and sea circulation.

Comparison of measured and modelled vertical profiles of sea temperature and salinity is shown in figure 8.

Comparison of modelled and measured hourly averaged circulation velocities (u and v components) is given in the form of graphical interpretation for the position of oceanographic station S-8 (Figs. 9 and 10).

The presentation of hourly averaged model current fields and E.Colli concentration fields for few characteristic situations during the analysed period (4.7.2008 – 22.8.2008), for depths of -2m, -8m, -16m, and -26m is given in Figures 11-16.

Model maximum E.Colli concentration fields at the depths of -2m, -8m, -10m, -16m, -20m, -26m, -30m, and -34m for the whole simulation period 4.7.2008 – 22.8.2008. are shown in Figure 17. Model maximum E.Colli concentration field in vertical profile P1-P2-P3 (see Fig. 17) for the whole simulation period 4.7.2008-22.8.2008. is given in figure 18.
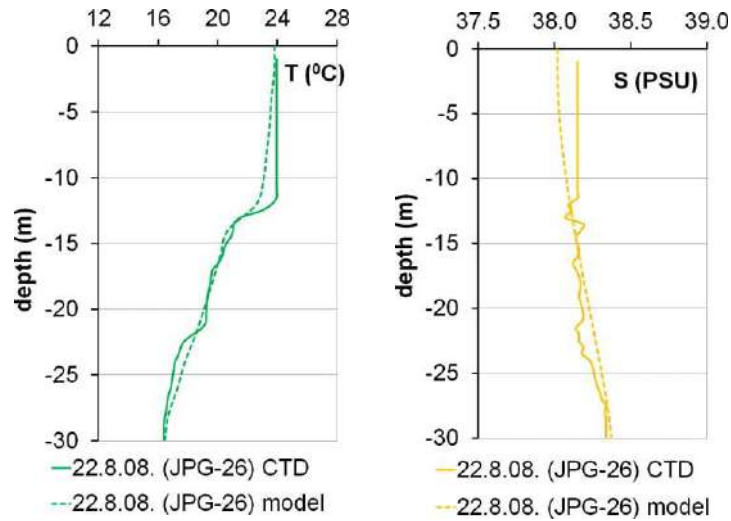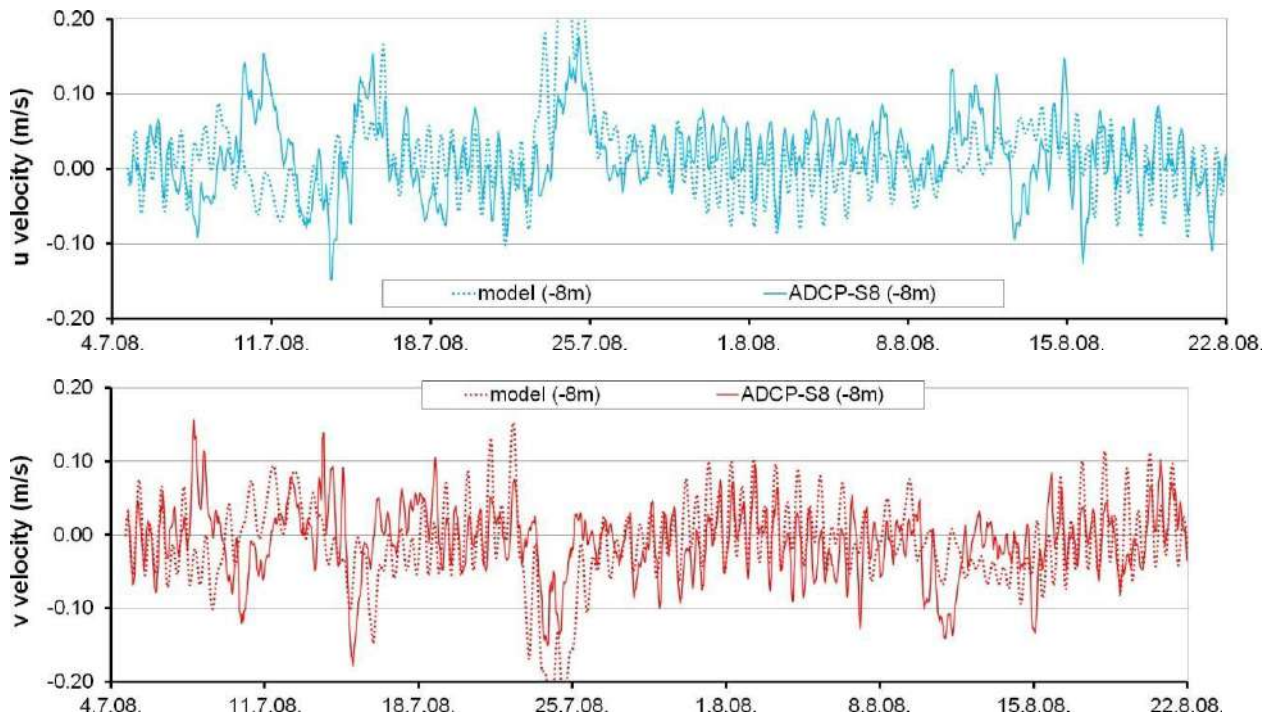

Figure 8 Comparison of measured and modelled vertical profiles of sea temperature and salinity for oceanographic station JPG-26 on 22.8.2008.

On the position of CTD station JPG-26, numerical model vertical profile of sea temperature follows measured profile throughout the sea water column. Measured vertical distributions of sea salinity are well interpreted by model in the bottom and intermittent layer. One can notice deflection of model salinity results from measured values in the sea surface layer above -12 meter depth, where model values are less than measured values.
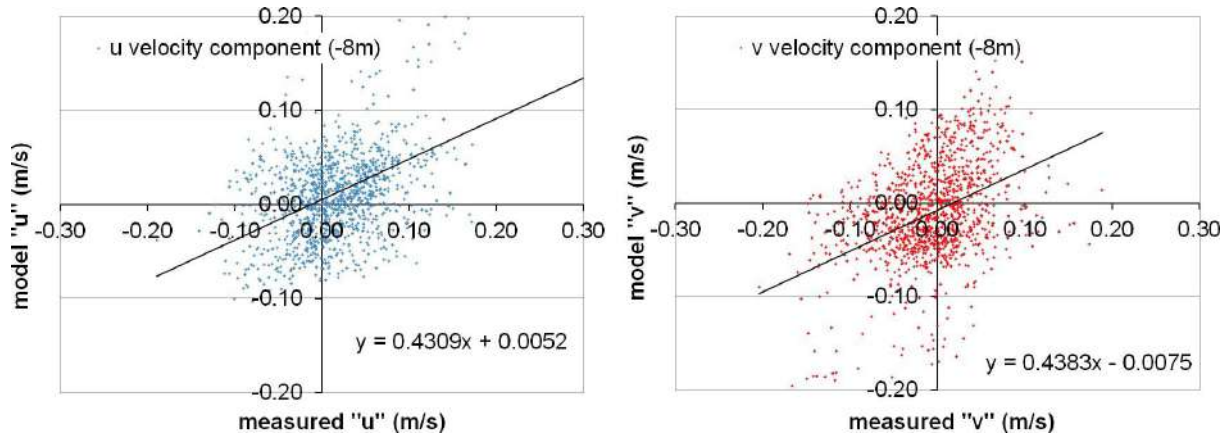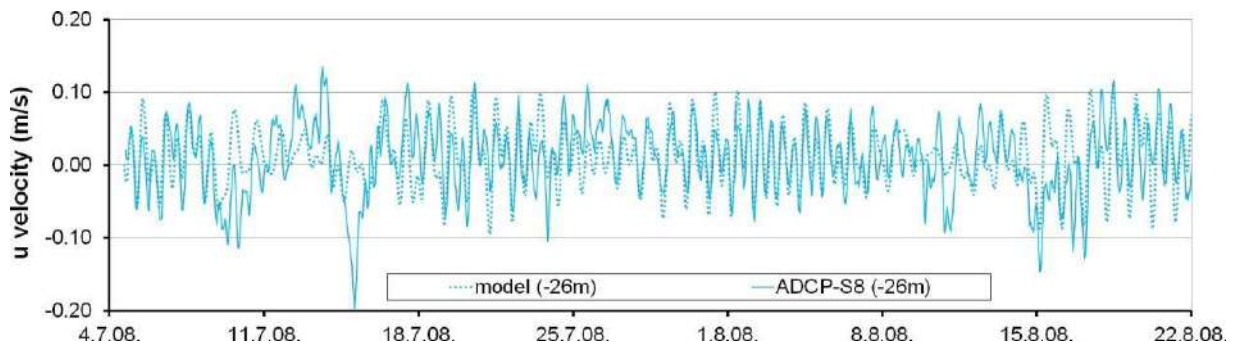
Figure 9 Comparison of measured and modelled velocity components for position of station S-8 at 8m depth

At the ADCP site S8 a relatively high degree of similarity between the measured and model values (Mike 3 FM) has been achieved for both sea current components. At the location of current meter site S8, the model values exceed the measured ones for both the u- and v- component of current velocity. Furthermore, this exceeding is somewhat more intensive in the surface layer than in the bottom layer. At the location of current meter site S8, periodic changes in the measured directions of flow are very well reproduced. The spatial domain of the numerical model covers the channel area in which the tidal signal as deterministic excitation has an important contribution in comparison with other flow generators due to which the very process of model calibration was facilitated, which in the end resulted in a relatively high degree of similarity between the measured and model values. Numerical model results are not of such degree of accuracy during the wind episodes, which is most probably a consequence of a certain error in Mike 3 fm model input data. Basically, it is primarily caused by the difference between the actual and model (ALADIN-hr) values of wind velocity and direction and its duration. Furthermore, in the event of bora wind occurrence, which is manifested through more pronounced periodic character, the 3-hour averaged value of wind intensity and direction obtained from the ALADIN-hr model cannot fully reproduce high-frequency energy exchange between the atmosphere and the sea. Also, one should be critical regarding the capabilities of numerical models that lose 'smoothness' of the flow field if the atmospheric input is of a very high time resolution.
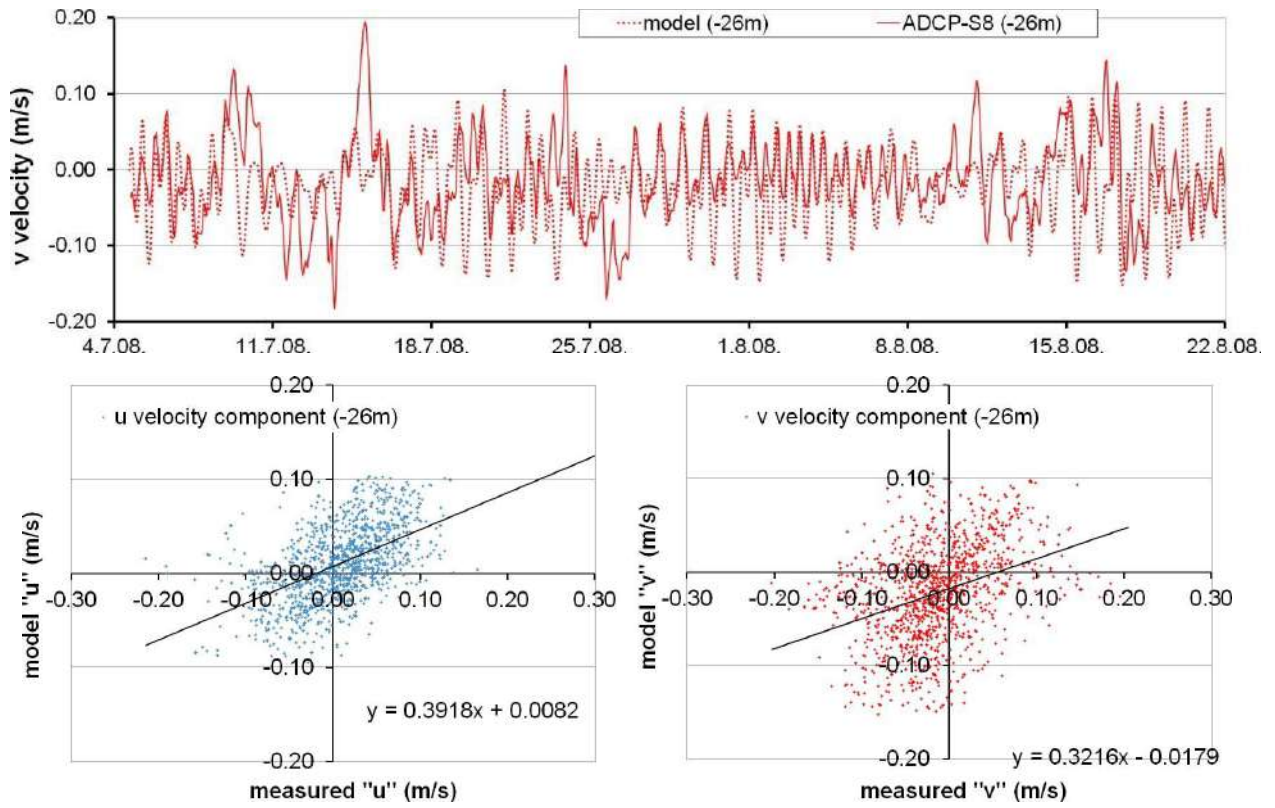
Figure 10 Comparison of measured and modelled velocity components for position of station S-8 at 26m depth
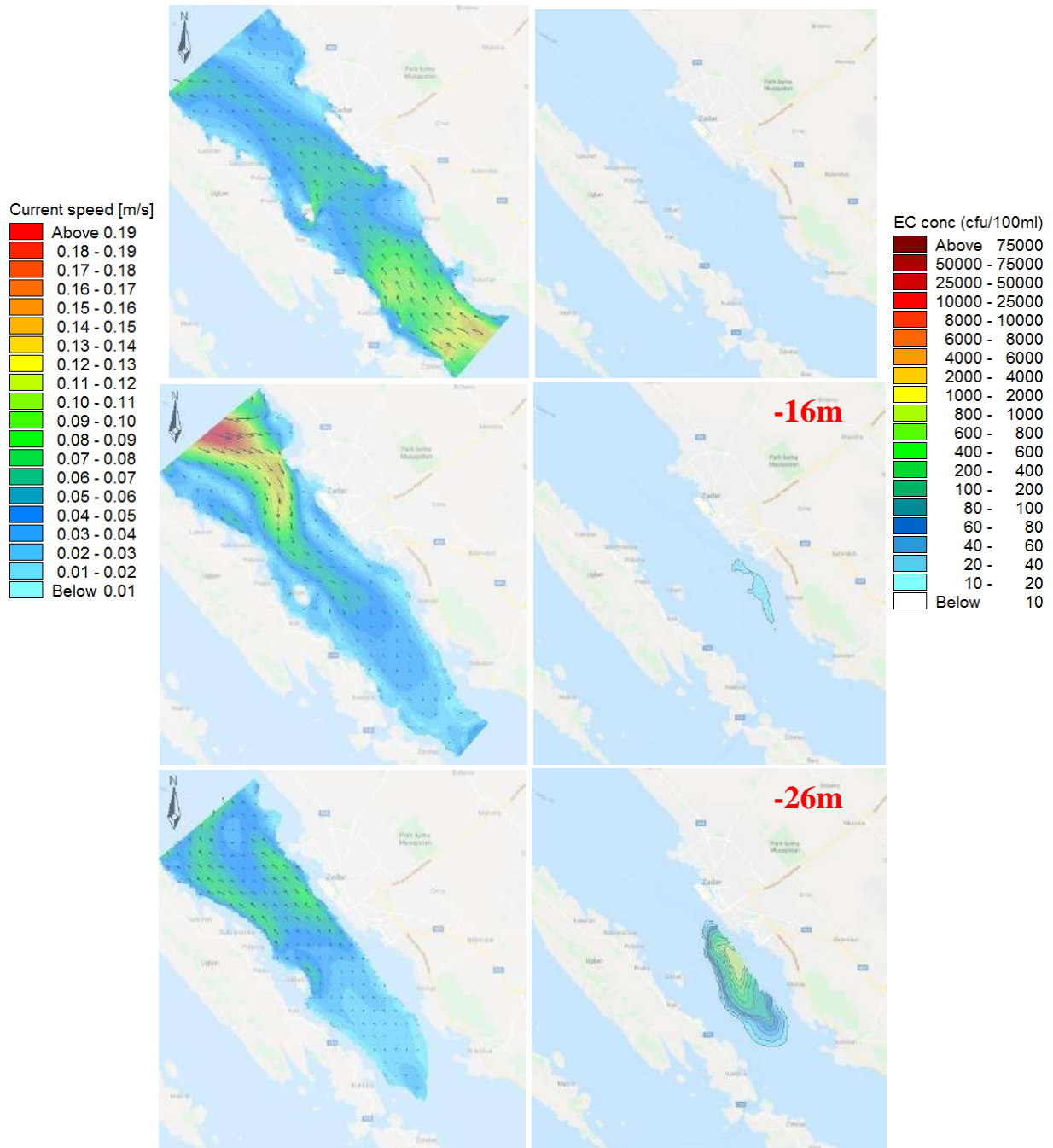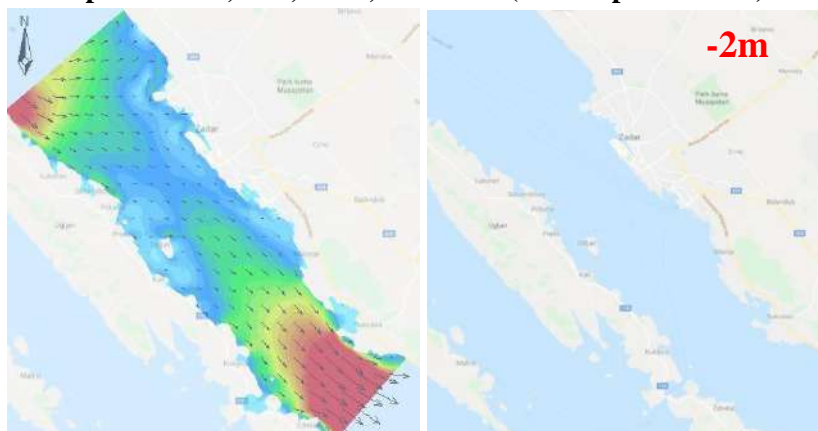
Figure 11 Hourly averaged model current fields (left) and EC concentration fields (right) for 13.7.2008 8:00 at the depths of -2m, -8m, -16m, and -26m (from top to bottom)
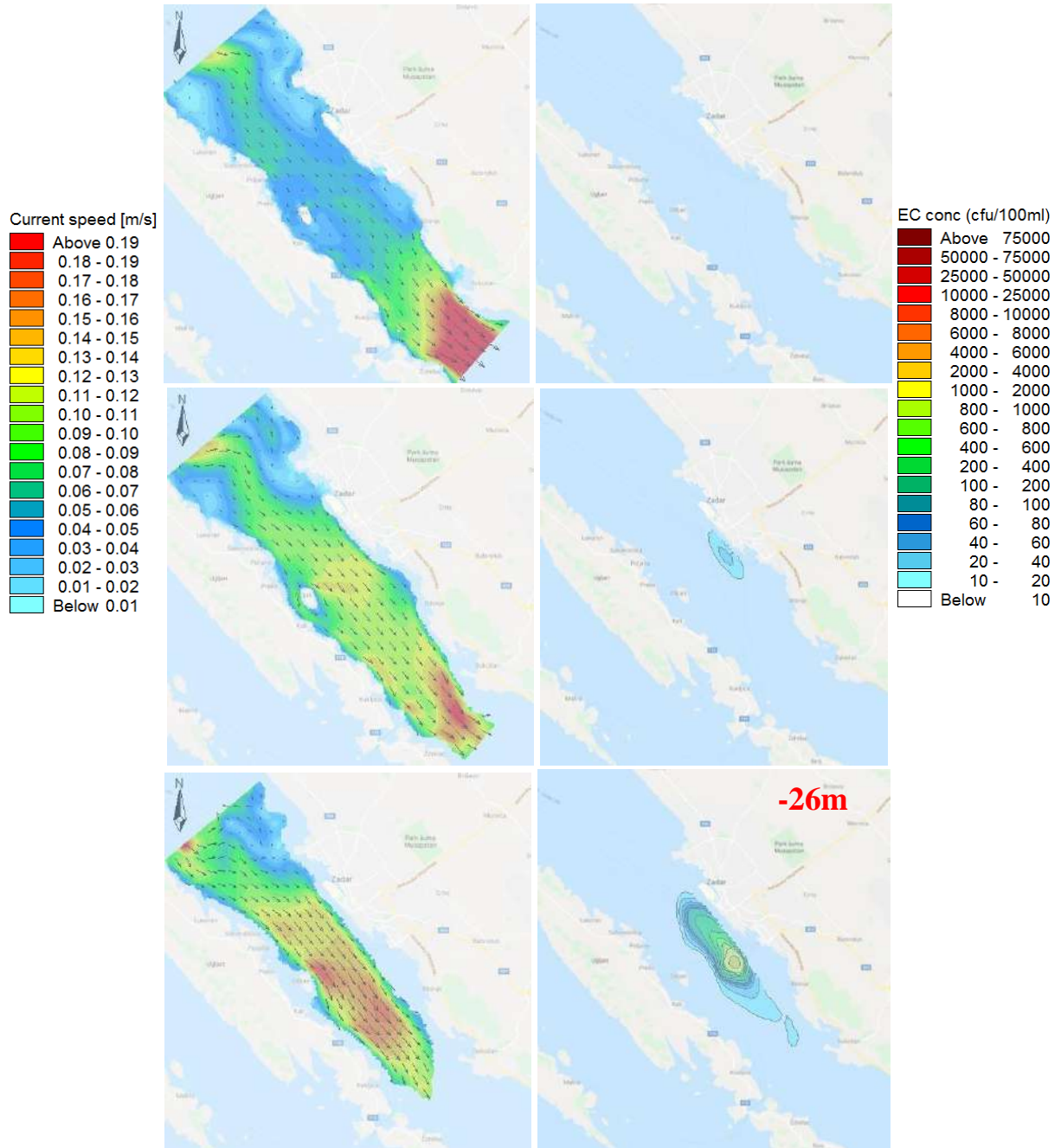
Figure 12 Hourly averaged model current fields (left) and EC concentration fields (right) for 18.7.2008 10:00 at the depths of -2m, -8m, -16m, and -26m (from top to bottom)
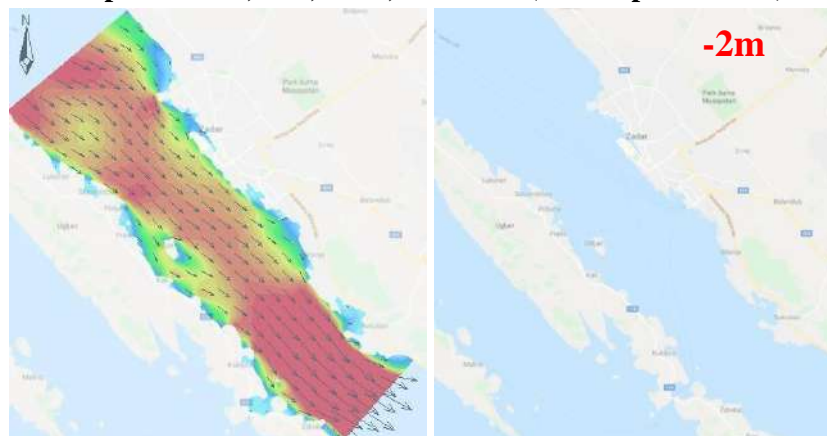
Figure 13 Hourly averaged model current fields (left) and EC concentration fields (right) for 19.7.2008 12:00 at the depths of -2m, -8m, -16m, and -26m (from top to bottom)
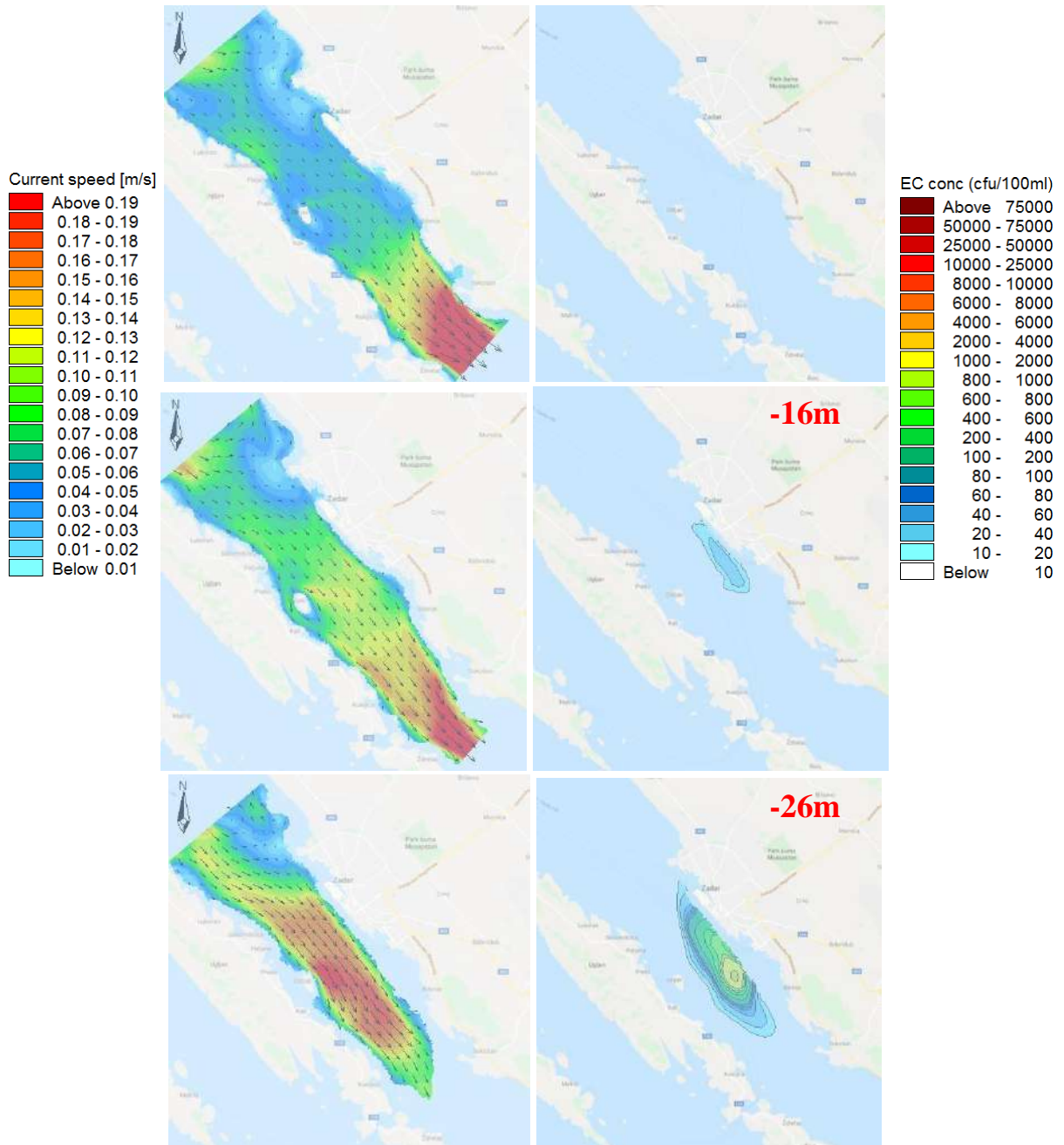
Figure 14 Hourly averaged model current fields (left) and EC concentration fields (right) for 21.7.2008 19:00 at the depths of -2m, -8m, -16m, and -26m (from top to bottom)

Figure 15 Hourly averaged model current fields (left) and EC concentration fields (right) for 23.7.2008 12:00 at the depths of -2m, -8m, -16m, and -26m (from top to bottom)
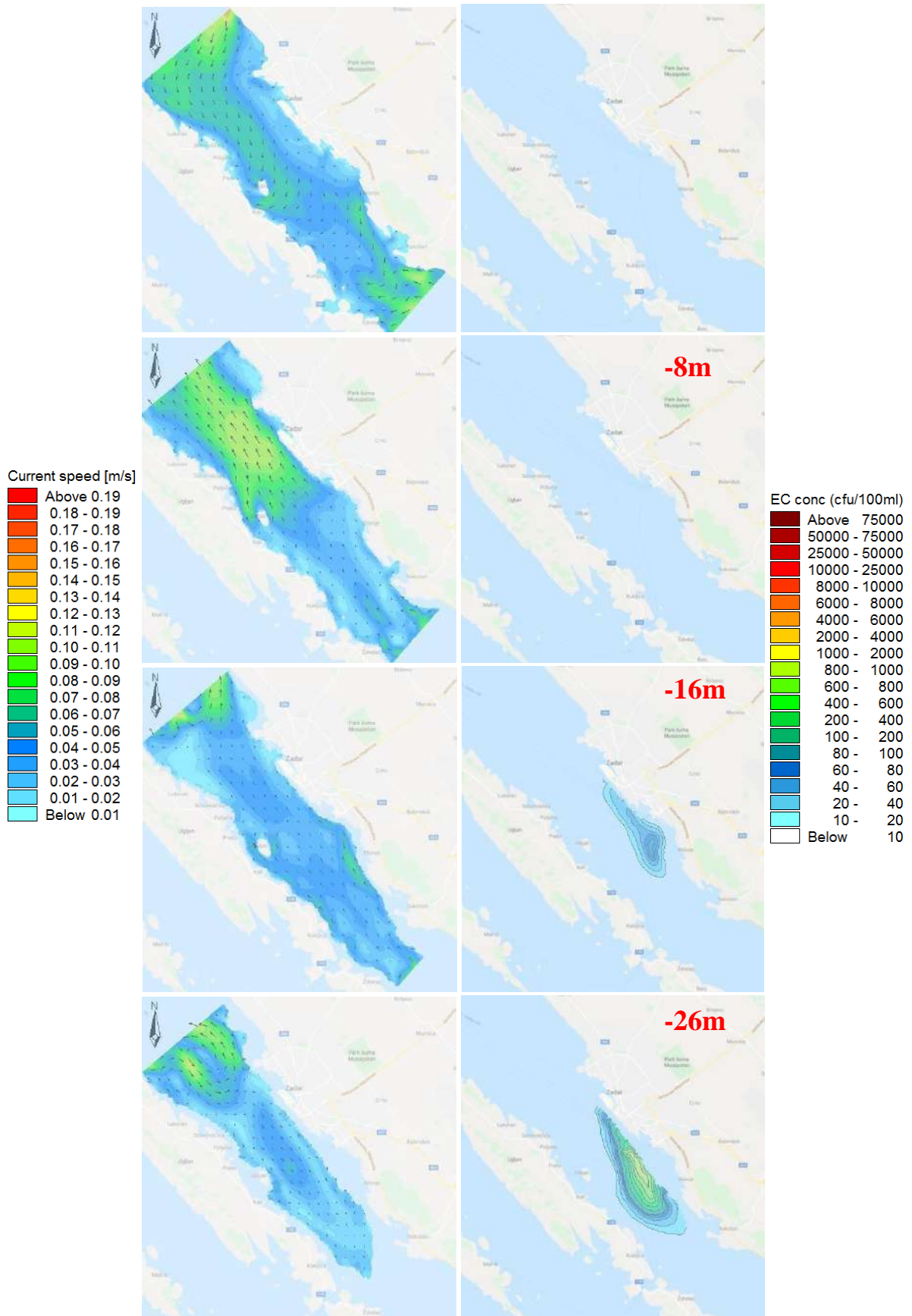
Figure 16 Hourly averaged model current fields (left) and EC concentration fields (right) for 25.7.2008 9:00 at the depths of -2m, -8m, -16m, and -26m (from top to bottom)
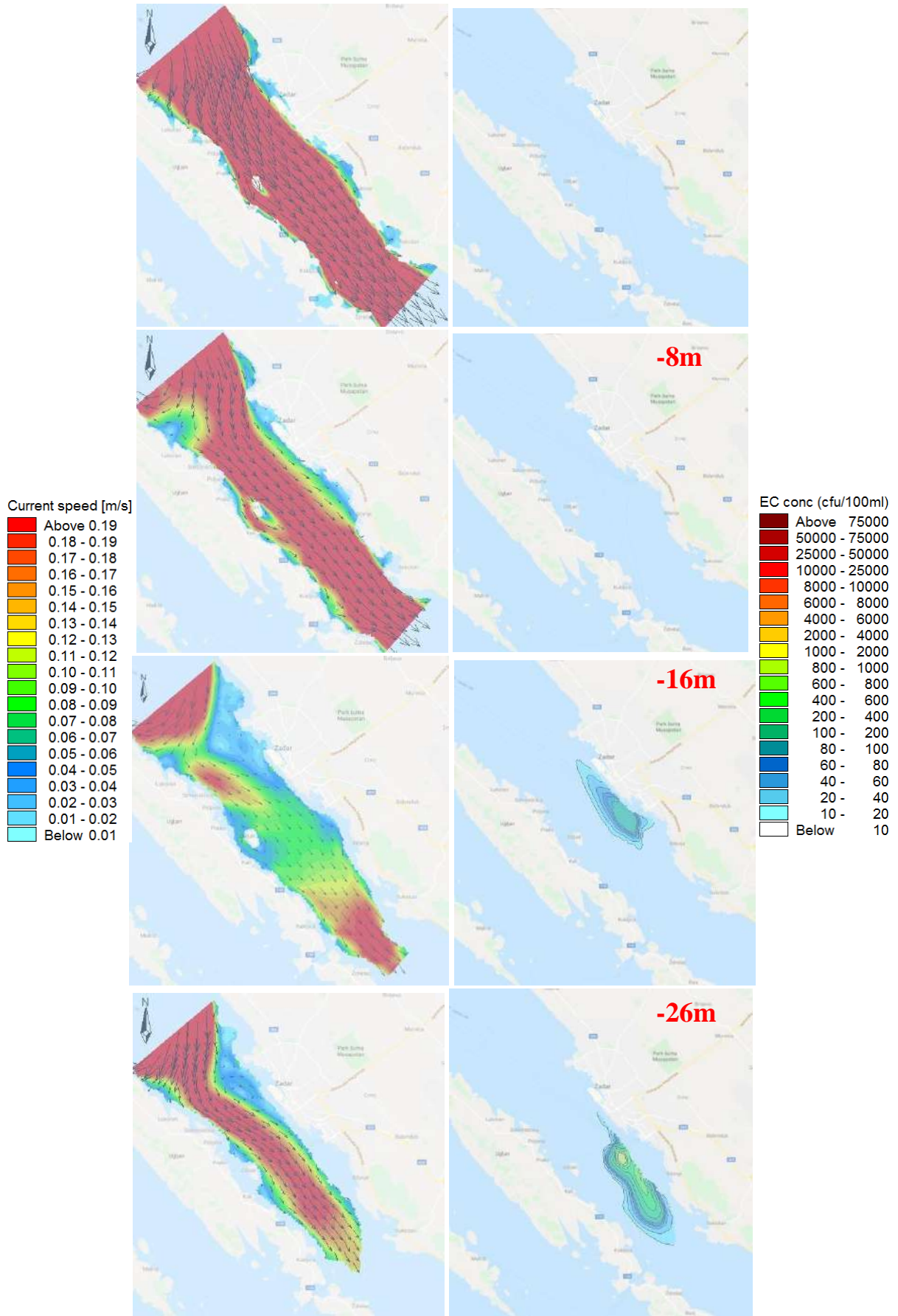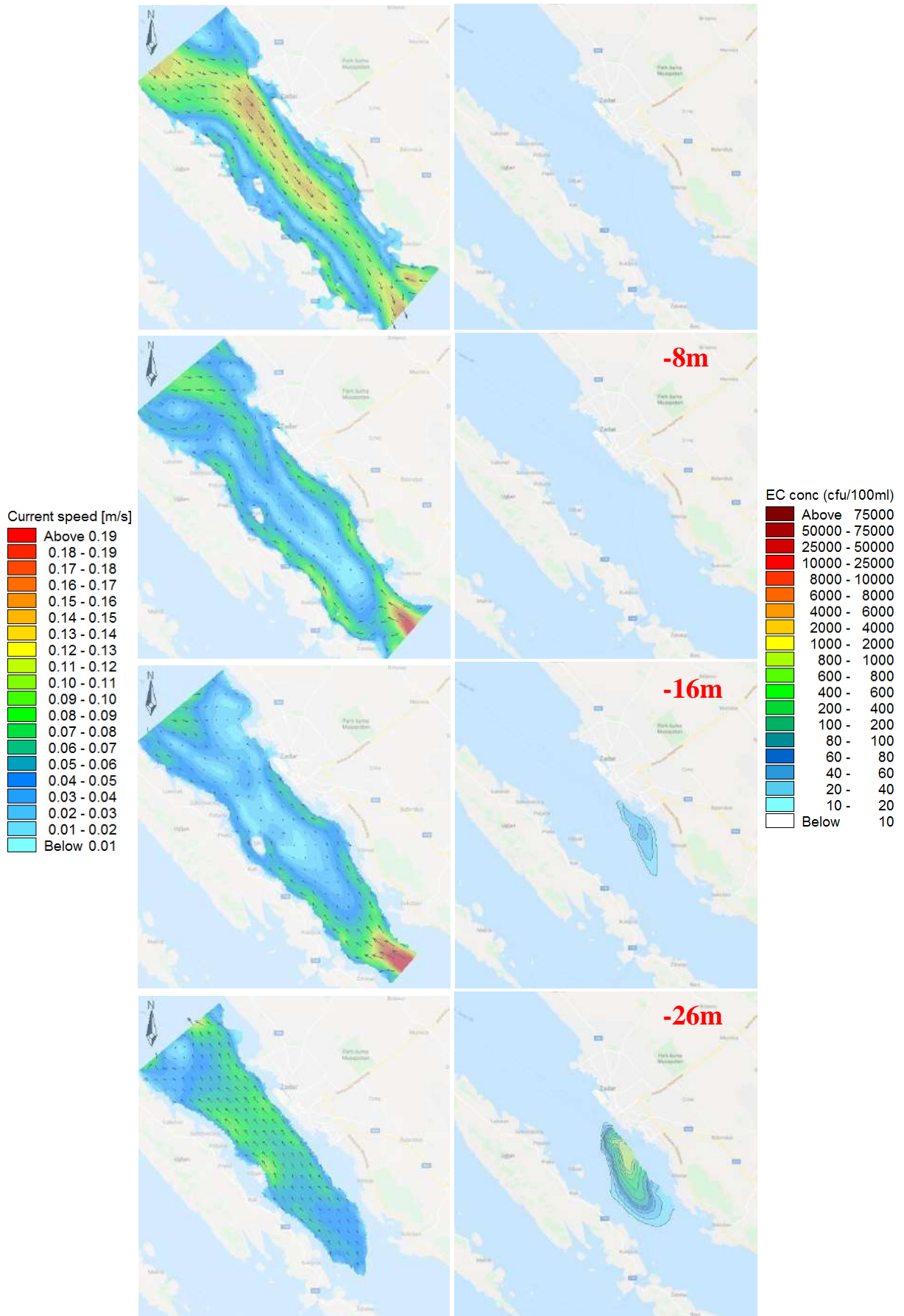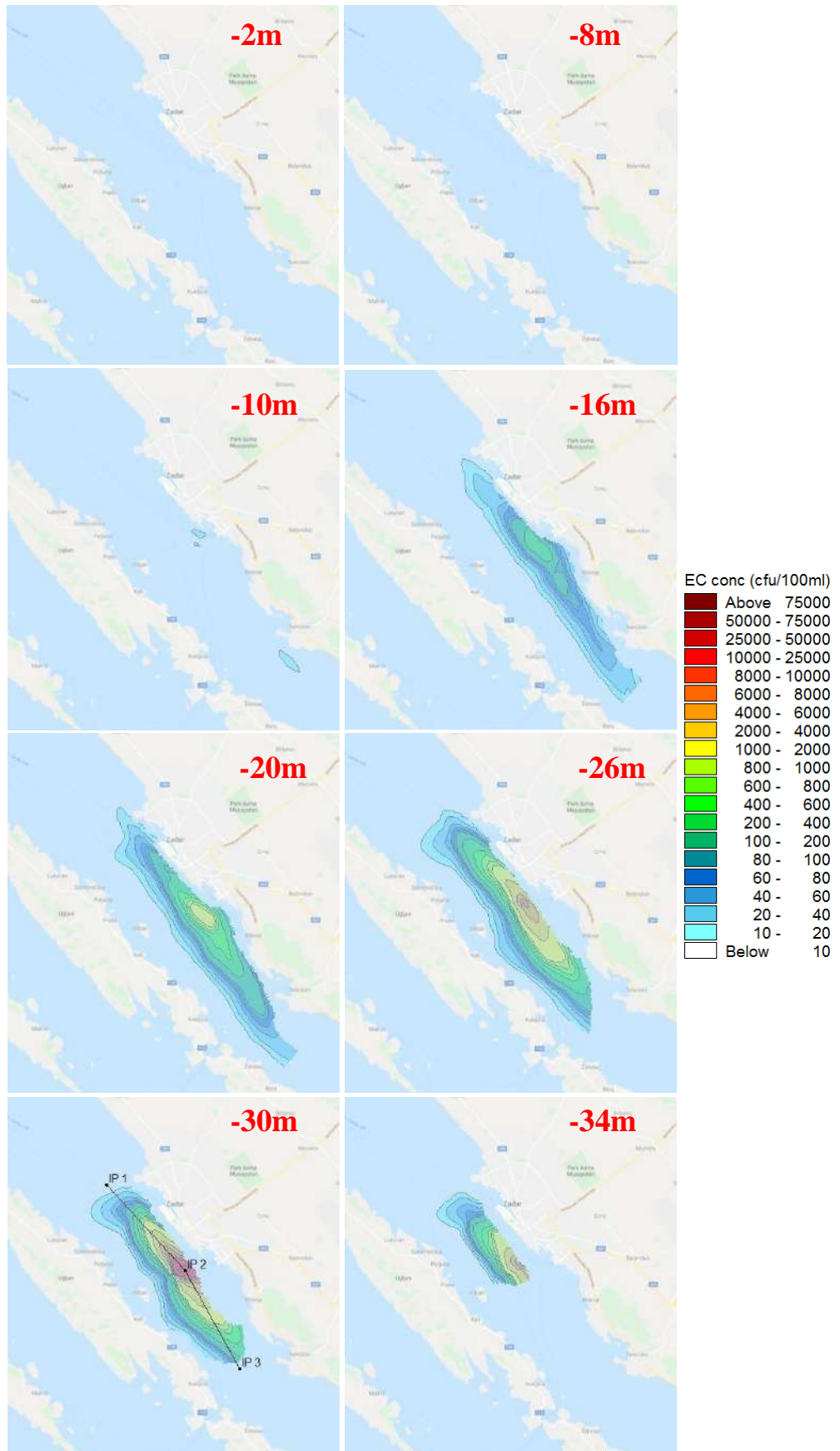
Figure 17 Model maximum E.Colli concentration fields at the depths of -2m, -8m, -10m, -16m, -20m -26m, -30m, and -34m for the whole simulation period 4.7.2008-22.8.2008.
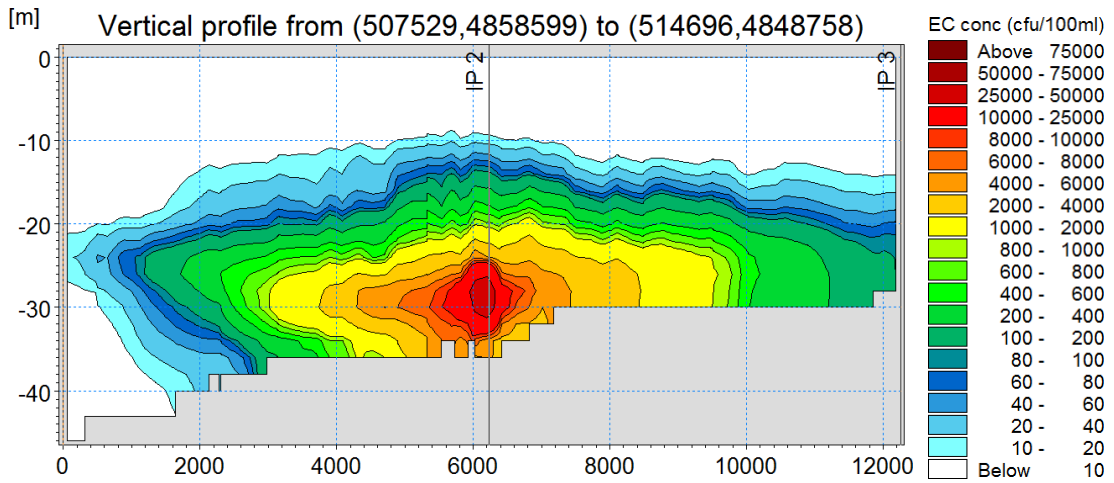
Figure 18 Model maximum E.Colli concentration field in vertical profile P1-P2-P3 (see Fig. 17) for the whole simulation period 4.7.2008-22.8.2008.

4. CONCLUSION

Circulation variability in the channal area off Zadar was reproduced with Mike 3fm modelling systems. Mike 3fm is a finite volume model and uses unstructured horizontal grid with resolution ranging from 350 m at the deeper part of the domain up to 35 m close to the coast. Model was forced with atmospheric and tidal forcing, along with the measured sea temperature and salinity fields on the model open boundaries. Atmospheric forcing was calculated from the output fields of the meteorological mesoscale model ALADIN-hr having 8 km horizontal resolution and 3 hour resolution in time using standard bulk formulation. Simulations covered the periods 4.7.2008-22.8.2008.

Current fields obtained by used modelling system (Mike 3 fm) are in agreement with the ADCP measurements performed in the area of the model spatial domain. The northwestward currents dominate in the surface layer, while in the lower layers of the channel topographically controlled gyres can be observed. Both measurements and numerical simulations indicate current reversal to souteastern direction in the coastal area off Zadar during summer. Modelled temperature and salinity profiles are of acceptable accuracy.

Resultant fields with spatial distribution of maximum E.Colli concentrations in model domain during the entire period covered by numerical analyses (4.7.2008. – 22.8.2008.) are presented in chapter 3. The continuous dynamics of spreading of effluent plumes is shown in animation files.

The ranges of Escherichia coli concentration according to which the sea water quality classification is carried out are defined on the basis of "Regulation on the bathing waters quality" (Croatian Official Gazette 73/08, Article 5),:

Escherichia coli (E.Colli)	<100 cfu/100ml	(excellent quality)
	101-200 cfu/100ml	(good quality)
	201-300 cfu/100ml	(satisfactory kvaliteta)

It should be noted that given national criterion is more than twice as strength as the criterion defined in the Bathing Water Directive 2006/7/EC.

The presented results show that the sea surface layer in the protected zone at 300m from the shore is of excellent quality (<100 cfu/100 ml) in the case of an existing stage of purification at WWTP Zadar - centar. Pollution plume lifting towards the sea surface is registered up to 13m depth (boundary concentration 100 cfu/100ml) during the July - August simulation period.

The appearance of stratification contributes to the retention of the effluent plume in the bottom layer. The complete homogenization of the vertical sea densities due to the windy episodes in the summer period, when the highest feacal pollution loads occur, has a very low probability of occurrence.

Finally, the results of numerical modeling have shown that waste waters treatment plant Zadar-centar, along with related submarine outfall, ensures preservation of valid lawcriteria regarding allowed concentrations of E.Colli.

REFERENCES

[1]   R. Sterneck, "Zur hydrodynamischen Teorie der Adriagezeiten", *Sitzungsberichte der Kaiserlichen Akademie der Wissenschaften in Wien*, Vol. 124, 1915, pp. 147-180.

[2]   R. Sterneck, "Gezeitenerscheinungen der Adria - II. Teil. Die theoretische Erklärung der Beobachtungstatsachen", *Denkschriften der Akademie der Wissenschaften in Wien*, Vol. 96, 1919, pp. 277-324.

[3]   A. Defant, *Annalen der Hydrographie und Maritimen Meteorologie*, Vol. 48, 1920, pp. 163-169.

[4]   E. Accerboni, B. Manca, "Storm surges forecasting in the Adriatic Sea by means of a two- dimensional hydrodynamical numerical model", *Boll. Geofis Teor. Appl.*, Vol. XV, 1973, pp. 3-22.

[5]   F. Stravisi, "A numerical experiment on wind effects in the Adriatic Sea", *Accademia Nazionale dei Lincei, Rendiconti della Classe di Scienze Fisiche, Matematiche e Naturali*, Ser. VIII, Vol. LII, 1972, pp. 187-196.

[6]   F. Stravisi, "Analysis of a storm surge in the Adriatic Sea by means of a two-dimensional linear model", *Accademia Nazionale dei Lincei, Rendiconti della Classe di Scienze Fisiche, Matematiche e Naturali*, Ser. VIII, Vol. LIV, 1973, pp. 243-260.

[7]   C. Finizio, S. Palmieri, A. Riccucci, "A numerical model of the Adriatic for the prediction of high tides at Venice" *Met. Soc.*, Vol. 98, 1972, pp. 86-104.

[8]   A.R. Robinson, A. Tomasin, A. Artegiani, "Flooding of Venice: Phenomenology and prediction of the Adriatic storm surge", *Met. Soc.*, Vol. 99, 1973, pp. 688-692.

[9]   M. Kuzmić, M. Orlić, M. Karabeg, Lj. Jeftić, "An investigation of wind-driven topographically controlled motions in the Northern Adriatic", *Estuar. Coastal Shelf Sci.*, Vol. 21, 1985, pp. 481-499.

[10] M.C. Hendershott, P. Rizzoli, "The winter circulation of the Adriatic Sea", *Deep-Sea Res.*, Vol. 23, 1976, pp. 353-370.

[11] M. Kuzmić, M. Orlić, "Wind induced vertical shearing - Alpex/Medalpex data and modelling excercise", *Annales Geophysicae B*, Vol. 5, 1987, pp. 103-112.

[12] M. Bone, "On topographic and wind vorticity effects in bora driven circulation in the North Adriatic", *Geofizika*, Vol. 4, 1987, pp. 129-135.

[13] M. Orlić, M. Kuzmić, Z. Pasarić, "Response of the Adriatic Sea to the bora and sirocco forcing", *Cont. Shelf Res.*, Vol. 14, 1994, pp. 91-116.

[14] D.C.Jr. Gordon, P.R. Boudreau, K.H. Mann, J.E. Ong, W.L. Silvert, S.V. Smith, G. Wattayakorn, F. Wulff, T. Yanagi, "Biogeochemical modelling guidelines", *LOICZ*, Vol. 5, 1995, Texel, The Netherlands, pp. 96.

[15] E. Hofmann, C. Lascara, "Overview of Interdisciplinary Modeling for Marine Ecosystems", In: K.H. Brink, A.R. Robinson (Eds.), *The Sea*, Vol. 10, 1998, pp. 507-540.

[16] J. McCarthy, A. Robinson, B. Rothschild, "Biological - physical interactions in the sea: emergent findings and new directions", In: A. Robinson, J. McCarthy, B. Rothschild (Eds.), *The Sea*, Vol. 12, 2002, pp. 1-17.

[17] K.L. Denman, "Modelling planktonic ecosystems: parameterizing complexity", *Prog. Oceanogr.*, Vol. 57, 2003, pp. 429-452.

[18] J. Baretta, W. Ebenhöh, P. Ruardij, "The European Regional Seas Ecosystem Model, a complex marine ecosystem model", *J. Sea Res.*, Vol. 33, 1995, pp. 233-246.

[19] J. Baretta-Bekker, J. Baretta, W. Ebenhoeh, "Microbial dynamics in the marine ecosystem model ERSEM II with decoupled carbon assimilation and nutrient uptake", *J. Sea Res.*, Vol. 38, 1997, pp. 195-212.

[20] M. Vichi, M. Zavatarelli, N. Pinardi, "Seasonal modulation of microbial - mediated carbon fluxes in the Northern Adriatic Sea", *Fisheries Oceanogr.*, Vol. 7, 1998, pp. 182-190.

[21] M. Zavatarelli, J. Baretta, J. Baretta-Bekker, N. Pinardi, "The dynamics of the Adriatic Sea ecosystem; an idealized model study", *Deep-Sea Res.*, Vol. 47, 2000, pp. 937-970.

[22] M. Vichi, P. Ruardij, J.W. Baretta, "Link or sink: a modelling interpretation of the open Baltic biogeochemistry", *Biogeosciences*, Vol. 1, 2004, pp. 79-100.

[23] C. Raick, E.J.M. Delhez, K. Soetaert, M. Gregoire, "Study of the seasonal cycle of the biogeochemical processes in the Ligurian Sea using a ID interdisciplinary model", *J. Mar. Syst.*, Vol. 55, 2005, pp. 177-203.

[24] M. Vichi, W. May, A. Navarra, "Response of a complex ecosystem model of the northern Adriatic Sea to a regional climate change scenario", *Clim. Res.*, Vol. 24, 2003, pp. 141- 159.

[25] Vilibić, I., Orlić, M., Surface Seiches and Internal Kelvin Waves Observed Off Zadar (East Adriatic). *Estuarine, Coastal and Shelf Science*, 48 (1999), pp. 124-136.

[26] Bone, M., Development of a non-linear levels model and its application to bora-driven circulation on the Adriatic shelf. *Estuarine, Coastal and Shelf Science,* 37 (1993), pp. 475- 496.

[27] Orlić, M., Dadić, V., Grbec, B., Leder, N., Marki, A., Matić, F., Mihanović, H., Beg Paklar, G., Pasarić, M., Pasarić, Z.,Vilibić, I., Wintertime buoyancy forcing, changing seawater properties and two different circulation systems produced in the Adriatic. *Journal of Geophysical Research*, 112(C3) (2007), C03S07, doi:10.1029/2005JC003271.

[28] Fischer, H.B., List, E.J., Koh, R., Imberger, J., Brooks, N.H. (1979.): *Mixing in Inland and Coastal Waters*, Academic Press, 1979.

[29] Cushman-Roisin, B., Gualtieri, C., Mihailović, D.T., 2008, *Environmental fluid mechanics: Current issues and future outlook, In: Fluid Mechanics of Environmental Interfaces* (C. Gualtieri and D.T. Mihailović Eds.), Taylor & Francis, 2008, 1-13.

[30] Akar, P. J., Jirka, G. H. (1994): Buoyant Spreading Processes in Pollutant Transport and Mixing, Part 1: Lateral spreading with ambient current advection, *Journal of Hydraulic Research*, 32(6), 427-439.

[31] Akar, P. J., Jirka, G. H. (1994): Buoyant Spreading Processes in Pollutant Transport and Mixing, Part 2: Upstream spreading in weak ambient current, *Journal of Hydraulic Research*, 33(1), 24-37.

[32] Wood, I.R., Bell, R.G., Wilkinson, D. L., 1993, *Ocean Disposal of Wastewater*, Advanced Series on Ocean Engineering – Volume 8, World Scientific, London. 425 pp.

[33] Pun, K.L., Davidson, M. J., 1999, *On the behaviour of advected plumes and thermals*, Journal of Hydraulic Research, 37(4), 296-311.

[34] Featherstone, R.E. (1984): Mathematical models of the discharge of wastewater into a marine environment, *In: James, A. (Ed.), An Introductory to Water Quality Modelling*, first ed. Wiley, Chichester, 150–162.

[35] Turner, J.S. (1986): Turbulent entrainment: the development of the entrainment assumption, and its application to geophysical flows, *J. Fluid Mech.*, 173, 431–471.

[36] Fan, L.N., Brooks, N.H. (1966): Horizontal jets in stagnant fluid of other density, *J. Hydraul. Divn.*, ASCE 92, 423–429.

[37] W. Rodi, "Examples of calculation methods for flow and mixing in stratified fluids", *Journal of Geophysical Research*, Vol. 92, 1987, pp. 5305-5328.

[38] C. Galos, *Seasonal circulation in the Adriatic Sea*, M.S. thesis, Dartmouth Coll., Hanover, 2000.

[39] I. Janeković, M. Kuzmić, "Numerical simulation of the Adriatic Sea principal tidal constituents", *Ann. Geophys.*, Vol. 23, 2005, pp. 3207–3218.

[40] P.C. Courtier, J.F. Freydier, F. Geleyn, M. Rochas, "The ARPEGE project at METEO- FRANCE", *Proceedings from the ECMWF workshop on numerical methods in atmospheric models*, Vol. 2, Reading, England, 1991, pp. 193-231.

[41] E. Cordoneanu, J.F. Geleyn, "Application to local circulation above the Carpathian-Black Sea area of a NWP-type meso-scale model", *Contributions to Atmospheric Physics*, Vol. 71, 1998, pp. 191-212.

[42] N. Brzović, "Factors affecting the Adriatic cyclone and associated windstorms", *Contributions to Atmospheric Physics*, Vol. 72, 1999, pp. 51-65.

[43] N. Brzović, N. Strelec-Mahović, "Cyclonic activity and severe jugo in the Adriatic", *Physics and Chemistry of the Earth (B)*, Vol. 24, 1999, pp. 653-657.

[44] S. Ivatek-Sahdan, M. Tudor, "Use of high-resolution dynamical adaptation in operational suite and research impact studies", *Meteorol. Z.*, Vol. 13, 2004, pp. 99-108.

[45] Lee, C.W. Yee, A., Fang Ng, Bong, C.W., Narayanan, K., Sim, E.U.H., Ng, C.C. (2011): Investigating the decay rates of Escherichia coli relative to Vibrio parahemolyticus and Salmonella Typhi in tropical coastal waters, *Water Research*, 45(4), pp. 1561-1570.

[46] De Brauwere, A., De Brye, B., Servais, P., Passerat, J., Deleersnijder, E. (2011.): Modelling Escherichia coli concentrations in the tidal Scheldt river and estuary. *Water Res.*, 45, 2724–2738.

[47] Jorgensen, S., Bendoricchio, G. (2001.): *Fundamentals of ecological modelling*, Elsevier- academic press, 2001.

Attachment 2

WP 3.2 Modelling and mapping of the project areas (Split pilot sites)

1. INTRODUCTION

Numerical models have been used a lot to interpret various aspects of the Adriatic Sea dynamics. One of the earliest numerical calculations was made in pre-computer era by Sterneck [1] and [2] and Defant [3] who integrated the frictionless hydrodynamic equations to study the Adriatic tides. More intensive use of numerical models in investigations of the Adriatic Sea dynamics coincided with introduction of computers in oceanography in the early 1970s. First computer model was made by Accerboni and Manca [4] in their study of the Adriatic tides. Early Adriatic computer models did not attempt to simulate the circulation but were simpler, storm-surge models with homogeneous density designed to calculate sea-surface elevation in response to wind events [5]-[9]. Particular attention was given to the simulation of bora storms and to prediction of flooding at Venice. Next important step in the numerical simulations in the Adriatic was made by Hendershott and Rizzoli [10]. They used a vertically integrated model to show the importance of topography upon the spreading of the deep water mass formed on the continental shelf of the northern Adriatic. In the late 1980s numerical modelling was concentrated on wind- driven circulation in the northern Adriatic [11]-[13] with particular attention paid to the response to bora events. Since then, there have been many regional and local model studies, utilizing *in situ* measurements and/or remote sensing techniques.

Contemporary modelling systems for the Adriatic Sea have been developed mostly within the framework of international project, e.g. *Project Adricosm*, *Mediterranean Forecasting System Pilot Project* etc. Basically, modern modelling system with realistic forcing consists of a hierarchy of more numerical models coupled among each other by nesting techniques, to downscale the larger scale flow field to highly resolved coastal scale fields. *In situ* and remote sensing data are used to evaluate modelling system performance, in particular a set of collected CTD measurements and satellite derived sea surface temperature measurements (SST), assessing a full three-dimensional picture of modelling systems quality.

For example, numerical modelling system launched within *Project Adricosm* (2001-2005) was set up in order to make an accurate forecast of short-term variability in the circulation of the Adriatic Sea, also giving some attention to the relevant processes in coastal areas. *In situ* measurements of individual parameters related to the atmosphere (meteorological parameters) and the sea (physical, chemical, and biological parameters), and their temporal and spatial sampling dynamics were as follows: *in situ* VOS data (temperatures profiles with monthly sampling frequency), CTD data (temperature, salinity and oxygen collected bi-weekly), satellite data (SST at high resolution and surface chlorophyll - *SeaWiFS*), buoy data (temperature, salinity, oxygen, pH, light transmission and current velocity) and atmospheric forcing data (wind velocity, air temperature, dew point temperature and cloud cover).

Other recently launched operational sea circulation modelling systems for the Adriatic region also utilize *in situ* measurement as verification tool, with above mentioned data sets collected only in the open sea region. *In situ* measurements obtained in the eastern part of the Adriatic (channel region), e.g. permanent ADCP recording, were not included in model verification procedures. Numerical models of ecosystems can also be used as tools for forecasting and evaluating the influence of human activities, or for analyzing future changes to an ecosystem that may take place under the influence of external factors [14]. Biogeochemical models representing trophic and chemical interactions in the marine system have been discussed largely in the past 20 years [15]-[17], particularly focusing on a biomass-based description of the pelagic system. The biogeochemical rates of change are outlined starting from the parameterizations of the *European Regional Seas Ecosystem Model* (ERSEM) [18], [19] which was the first comprehensive ecosystem model to include physiological considerations in the definition of the divergence of material fluxes. On the other hand several implementations of this model have shown the skill of this approach, both in coastal areas with large land-derived inputs but also in the oligotrophic Mediterranean regions [20]-[23]. The same approach has also been used in the context of climate studies, particularly to capture and analyze climate variability in the Adriatic Sea [24]. A direct descendant of ERSEM, the *Biogeochemical Flux Model* (BFM), is now being developed in the framework of the EU project MFSTEP (*Mediterranean Forecasting System towards Environmental Predictions*) and applied to the whole Mediterranean basin and sub-regional seas.

Existing ecology modelling systems for the Adriatic Sea are validated and verified only on *in situ* measurement and remote sensed data collected in the open sea region, excluding the data sets obtained from monitoring campaigns undertaken within eastern part of the Adriatic (channel region).

During the implementation of *Phase I of The Adriatic Sea Monitoring Program* (hereafter *JP-07/09*), for the very first time, the current meter sites (25) and physical-biology-chemistry sites (45) were located at relatively small distances from the shore. *Phase I* of *JP-07/09* has already set up measurement necessary for the design of the models aimed to the analysis of some principal components of the sea water (coastal or marine water) quality in the eastern part of Adriatic Sea. For example, results of measurements within *JP-07/09* can be used for numerical modeling implementation (calibration) in the assessment of the impact of planned wastewater treatment facilities. The changes in the marine ecosystem are brought about by the discharge of effluents, in particular the treated municipal fecal wastewater. However, it should be pointed out that wastewater discharge is not the only form of pollution of the coastal parts of the Adriatic Sea.

In *JP-07/09* the following parameters were measured: sea temperature, salinity and density, sea currents, seawater transparency, dissolved oxygen, pH, nutrients (ammonium, nitrite, nitrate, orthophosphate, orthosilicate, total phosphorous, total nitrogen), biomass and phytoplankton composition (chlorophyll a), number of bacterial cells (direct microscopic counts), and fecal pollution indicators (fecal coliforms, fecal streptococci).

In this project the numerical analyses are focused on fecal pollution indicator transport, primarily E.Colli. The establishment of the model system of sea circulation and dynamics of E.Colli significantly relies on the results of monitoring within JP-07/09.

2. ESTABLISHING NUMERICAL MODELS OF SEA CIRCULATION AND E.COLLI TRANSPORT

Effluent transport phenomena in aquatic environment belong to the class of interdisciplinary problems (Fischer et al. 1979 [25]). Fluid mechanics traditional objective is focused on project solution optimization and analyzes of structure operability. On the other hand, geophysics fluid mechanics (meteorology, oceanography) is more oriented on the relevant processes comprehension and prediction on the broader temporal and spatial scales. Environmental fluid mechanics targets its primer major concern somewhere between those two extremes with the aim of assessing the potential environmental hazard impact and helping in decision making processes for the proposed project solutions (Cushman-Roisin et al. 2008 [26]).

Dominant forcing and their intensities in the mixing processes affecting the effluent plume on its pathway from the orifice of the diffuser to the arbitrary downstream profile are highly variable. Therefore, concept of separating of the far field and the near field zones with different dominant forcing is widely adopted (Fischer et al. 1979 [25]). In the case of the public sewage submarine outfall, near field domain in the vicinity of outfall diffuser, ranges from the inflow point up to the sea surface or neutral buoyancy layer where further effluent plume raising is interrupted and afterwards plume dynamics is mainly in the horizontal direction (Akar and Jirka 1994a [27], 1994b [28]). Therefore, integral solution of the problem is most commonly obtained through usage of combination of two structurally different numerical models. Plume propagation in the far field is modeled with 3D oceanographic numerical model using initial concentration fields calculated from the near field model (Akar and Jirka 1994a [27], 1994b [28], Wood et al. 1993 [29], Pun and Davidson 1999 [30]). Using described approach one can avoid high resolution numerical grid within the far field model required for resolving near field mixing process. That approach consists of two successive steps: a) temporal changes of vertical density distribution along the water column at the positions of the analyzed submarine outfall diffusers are obtained from 3D numerical model simulations; b) mixing processes in the near field are resolved using numerical model built up according Featherstone (1984) [31], with previously calculated vertical density profiles. More details about used near field numerical model are given in section 2.1.

2.1. Near field transport model for E.Colli

Near-field plume dynamics features were calculated with the use of the separate near-field numerical model, using information of the vertical density distribution previously calculated within 3D numerical model.

Near field effluent transport model is defined using set of differential equations for motion on steady control volume (Featherstone 1984 [31]). The core of the model consists of assuming initially effluent inflow through a circular nozzle opening and single buoyant jet or plume propagation without any interaction with other buoyant jets or plumes from adjacent nozzles.

Volume flux ϕ, mass flux ψ, specific momentum flux M, buoyancy flux B and specific buoyant force per unit length of a plume T are expressed with integral equations 1a-1e, where A represents a cross-sectional area of a plume orthogonal to the central trajectory, u represents velocity in the plume cross section, ρ density in the plume cross section, $\Delta\rho$ density deficit ($\Delta\rho = \rho_m - \rho$), ρ_m sea density and ρ_{m0} sea density at the position of diffuser nozzles.

$$\phi = \int_A u\,dA \quad ; \quad \psi = \int_A \rho u\,dA \quad ; \quad M = \int_A u^2 dA \qquad (1a,b,c)$$

$$B = g\int_A \left(\frac{\Delta\rho}{\rho_{m0}}\right) \div u\,dA \quad ; \quad T = g\int_A \left(\frac{\Delta\rho}{\rho_{m0}}\right) \div dA \qquad (1d,e)$$

The core of the model is contained in the definition of the rate of change for ϕ, ψ, M and B fields along the central trajectory path s of the stationary plume. Neglecting the influence of ambient current on the overall plume dynamic, specific momentum rate of change becomes zero in the horizontal direction (eq. 2a). The change in the specific momentum in the vertical direction is caused by buoyancy (eq. 2b). Volume flux and mass flux change along the path s due to ambient fluid entrainment through the outer contour of the plume are defined with equation 3 (Turner, 1986 [32]). Henceforth specific momentum and volume flux follow:

$$\frac{d}{ds}(M\cos\theta) = 0 \; ; \quad \frac{d}{ds}(M\sin\theta) = T \qquad (2a,b)$$

$$\frac{d\phi}{ds} = E = 2\pi b\alpha u(s) \qquad (3)$$

where $u(s) = u(s,r=0)$ is velocity along the central trajectory of plume; b radial distance from central trajectory to the position where velocity assumes the value of $u(s,r=b) = u(s,r=0)/e$; $\alpha=0.083$ entrainment constant (Featherstone, 1984); θ is angle of inclination of a tangent of a plume trajectory to the horizontal axis.

One assumes that velocity $u(s,r)$ and density deficit $\Delta\rho(s,r)$ follow Gauss's distribution in the

plume cross section, using constant $\lambda = 1,16$ in case of scalar transport.

$$u(s,r) = u(s)e^{-r^2/b^2} \quad ; \quad \Delta\rho(s,r) = \Delta\rho(s)e^{-r^2/(\lambda b^2)} \tag{4a,b}$$

Integration of equation 1 (eq. 5) and definition of the proportionality between dB/ds and ϕ (eq. 6) along the streamline result in:

$$\phi = \pi u(s)b^2(s) \quad ; \quad M = \frac{\pi u^2(s)b^2(s)}{2} \tag{5a,b}$$

$$B = \frac{\pi g \lambda^2 \Delta\rho(s)u(s)b^2(s)}{\rho_{m0}(1+\lambda^2)} \quad ; \quad T = \frac{\pi g \lambda^2 \Delta\rho(s)b^2(s)}{\rho_{m0}} \tag{5c,d}$$

$$\frac{dB}{ds} = \frac{g}{\rho_{m0}}\frac{d\rho_m}{ds}\phi \tag{6}$$

Substituting ϕ, M, B (eq. 5) in equations 2, 3, 6, and using some algebraic manipulations, one obtains the system of equations 7-11. Abbreviated character u and $\Delta\rho$ are used instead of $u(s)$ and $\Delta\rho(s)$ for the sake of simplicity:

$$\frac{du}{ds} = \frac{2g\lambda^2\Delta\rho}{\rho_{m0}u}\sin\theta - \frac{2\alpha u}{b} \tag{7}$$

$$\frac{db}{ds} = 2\alpha - \frac{g\lambda^2\Delta\rho\, b}{\rho_{m0}u^2}\sin\theta \tag{8}$$

$$\frac{d\theta}{ds} = \frac{2g\lambda^2\Delta\rho}{\rho_{m0}u^2}\cos\theta \tag{9}$$

$$\frac{d\Delta\rho}{ds} = \frac{(1+\lambda^2)}{\lambda^2}\frac{d\rho_m}{dz}\sin - \frac{2\alpha\Delta\rho}{b} \tag{10}$$

$$\frac{dx}{ds} = \cos\theta \quad ; \quad \frac{dz}{ds} = \sin\theta \tag{11a,b}$$

Dilution S is defined according Fan et al. (1966) [33],:

$$S(s) = \frac{4\lambda^2 u b^2}{(1+\lambda^2) u_0 d^2}$$

(12)

Integration of equation 7-11 begins where Gaussian profile (eq. 4) are fully developed e.g. at a distance of s_0=6,2d (Featherstone 1984). Initial velocity $u(s=s_0=6,2d)$ equals the mean exit velocity at diffuser nozzle $4\phi_0/(\pi d^2)$, while initial plume radius is obtained from conservation of momentum $b_0 = d / \sqrt{2}$.

The initial deflection of nozzle axis from horizontal plane θ_0 retains the same value up to the distance s_0 or $\theta(s=s_0=6,2d)=\theta_0$. The value $\theta_0=0^0$ is used in the scope of numerical simulations, representing the case of horizontal nozzle set-up. Initial density difference at s_0 is assumed with equality $\Delta\rho(s=s_0=6,2d) = \Delta\rho_0 = [(\rho_{0m}-\rho_0)(1+\lambda^2)/(2\lambda^2)]$, initial coordinates of central plume trajectory with $x(s=s_0=6,2d)=x_0=s_0\cos\theta_0$ or $z(s=s_0=6,2d) = z_0 = s_0\sin\theta_0$ and initial dilution with $S(s=s_0=6,2d) = S_0 = 2\lambda^2/ (1+\lambda^2)$.

For solving the system of equations and in order to minimize local errors in the near field model Runge-Kutta 4. order method with variable spatial step was used. Model stops with integration when effluent plume reach the recipient surface or exceeds neutral buoyancy level.

Conglomerations have different degrees of public drainage system development with respective water treatment facilities and submarine outfalls. All cities and municipalities that already have the developed public drainage system (*Eko Kaštelanski zaljev*) or the planning documents on the implementation of the public sewerage system (*Projekt Jadran*) were treated in a way that the respective discharge rates and concentrations are discharged at the diffuser section of the related submarine outfall (Figure 1).
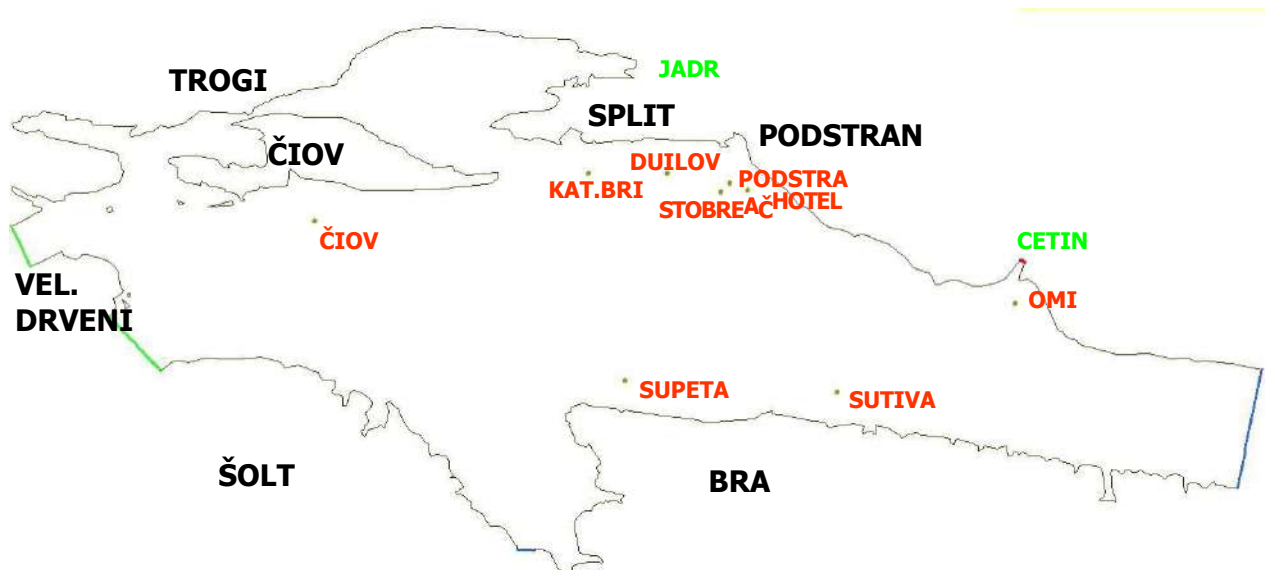

Figure 1 Locations of diffuser sections of the submarine outfalls of the existing public sewerage systems

Relevant data about main working characteristics of submarine outfalls are given in Figure 3. For better physical description of effluent spreading, caused by common operation of submarine outfalls, non-stationary mode which use working pulses, have been implemented in numerical model (Fig. 3). Initial concentration of $4*10^6$ cfu/100ml was used for all modeled submarine outfalls. Other possible sources of FC contamination were not taken into consideration.
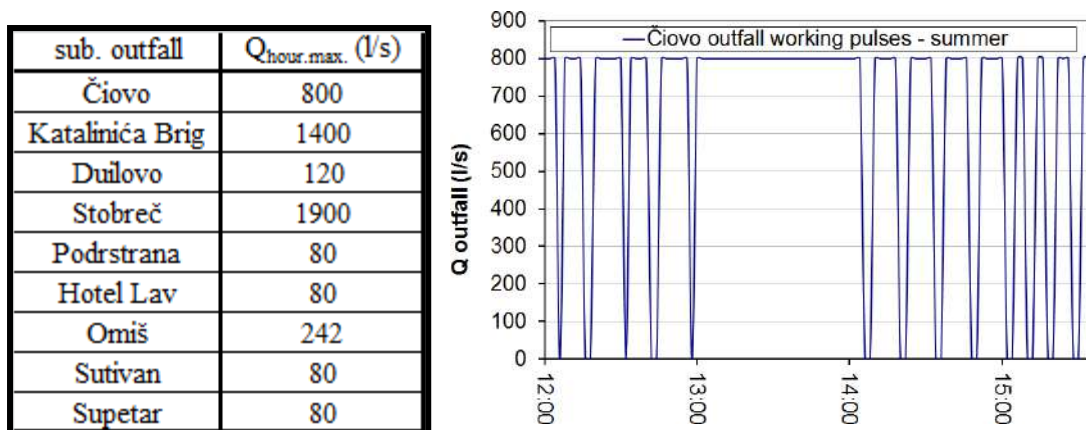
sub. outfall	$Q_{hour.max.}$ (l/s)
Čiovo	800
Katalinića Brig	1400
Duilovo	120
Stobreč	1900
Podrstrana	80
Hotel Lav	80
Omiš	242
Sutivan	80
Supetar	80

Figure 2 Main working characteristics of analyse submarine outfalls (left) and outfall discharge in nonstationary working mode (pulses) for sequence of characteristic "summer" day for Čiovo outfall (right)

2.2. *Sea circulation model (Mike 3)*

The modelling system Mike 3 (www.dhigroup.com) has been developed for applications within oceanographic, coastal and estuarine environments. The Hydrodynamic module is the basic computational component of the entire Mike 3 modelling system providing the hydrodynamic basis for the transport process.

The hydrodynamic Module is based on the numerical solution of the three-dimensional incompressible Reynolds averaged Navier-Stokes equations (RANS). Thus, the model consists of continuity, momentum, temperature, salinity and density equations and is closed by a turbulent closure scheme. The Hydrodynamic Module also calculates the resulting currents and distributions of salt, temperature, subject to a variety of forcing and boundary conditions. Baroclinic effect due to salt and temperature variations, and turbulence are considered as subordinated to the HD module. The density is assumed as a function of salinity and temperature, so the transport equations for the temperature and/or salinity are solved simultaneously. Calculated temperature and salinity are feed-back to the hydrodynamic equations buoyancy forcing induced by density gradients.

Decomposition of the prognostic variables into a mean quantity and a turbulent fluctuation leads to additional stress terms in the governing equations to account for the non-resolved processes both in time and space. By the adoption of the eddy viscosity concept these effects are expressed through eddy viscosity and the gradient of the mean quantity, thus the effective shear stresses in the momentum equations contain the laminar stresses and the Reynolds stresses (turbulence). The effects of rivers are included in the simulation through as sources, taking into account the

contribution to the continuity equation and the momentum equations.

The heat in the water can interact with the atmosphere through heat exchange. The heat exchange is calculated on the basis of the four physical processes: the long wave radiation, the sensible heat flux (convection), the short wave radiation, the latent heat flux (evaporation). For the calculation of heat exchange influences the specification of air temperature, relative humidity and clearness coefficient as time variable series are utilized. Furthermore, for the latent heat flux constants in Dalton's and Sun constants in Angstrom's law are defined and together with the time displacement and the local standard meridian for the time zone incorporated in the calculation procedure. Heating by short wave radiation in the water column is also included. The short wave penetration which is dependent on the visibility is specified through light extinction coefficient.

The turbulence module is invoked from the specification of vertical eddy viscosity. The turbulence model is based on a standard k-ε model [39]. This model uses transport equations for the turbulent kinetic energy - k and its dissipation - ε.

The hydrodynamics module of Mike 3 makes use of the so-called Alternating Direction Implicit (ADI) technique to integrate the equations for mass and momentum conservation in the space-time domain. The equation matrices, which result for each direction and each individual grid line, are resolved by a Double Sweep (DS) algorithm. Discretized on the Arakawa C-grid aiming at a second order accuracy on all terms, i.e. „second order"in terms of the discretization error in a Taylor series expansion. For analysis of transported fields 3D QUICKEST-SHARP scheme is used. This scheme belongs to a group of so-called CWC schemes (Consistency With Continuity), designed to be consistent with the continuity equation of the HD module. In most three-dimensional models the fluid is assumed incompressible. However, using the divergence-free (incompressible) mass equation, the set of equations will inevitably form a mathematical ill-conditioned problem. In most models this is solved through the hydrostatic pressure assumption whereby the pressure is replaced by information about the surface elevation. In order to retain the full vertical momentum aguation an alternative approach has been adopted in Mike 3. This approach is known as the artificial compressibility method in which an artificial compressibility term is introduced whereby the set of equations mathematically speaking becomes hyperbolic dominated.

3D numerical model of sea circulation, as a basis for further analyses of E.Colli transport in far-field, is established with spatial domain that covers the area of Split and Brač channel (Fig. 3). The simulations are carried out for the period from 10 May 2008 to 25 August 2008. The numerical model domain is discretized (calculation mesh) with equidistant spatial step $\Delta x = 169m$ and $\Delta y = 229m$. Near the respective open boundaries (Fig. 3) there is at least one monitoring station from which it is possible to collect data on boundary conditions (Fig. 4).
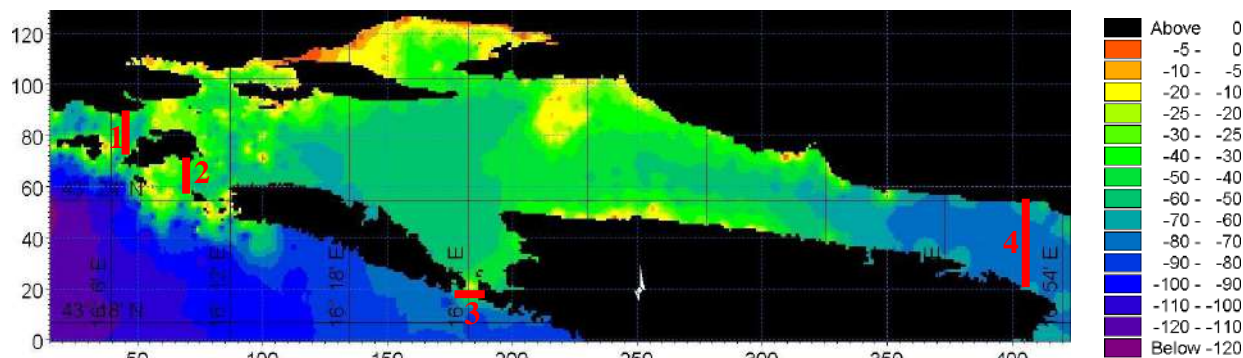
Figure 3 Spatial domain of model 1 (Mike 3, open boundaries are indicated with numbers 1 - 4)

Figure 4 Locations of oceanographic stations during the implementation of the *Adriatic Sea Monitoring Program* (*JP-07/09*)

Numerical integration of the circulation models started on 10 May 2008 by initiation with the sea temperature and salinity fields at standard oceanographic depths from the oceanographic database of Dartmouth College (Fig. 5, Dartmouth Adriatic Data Base – DADB [34]).
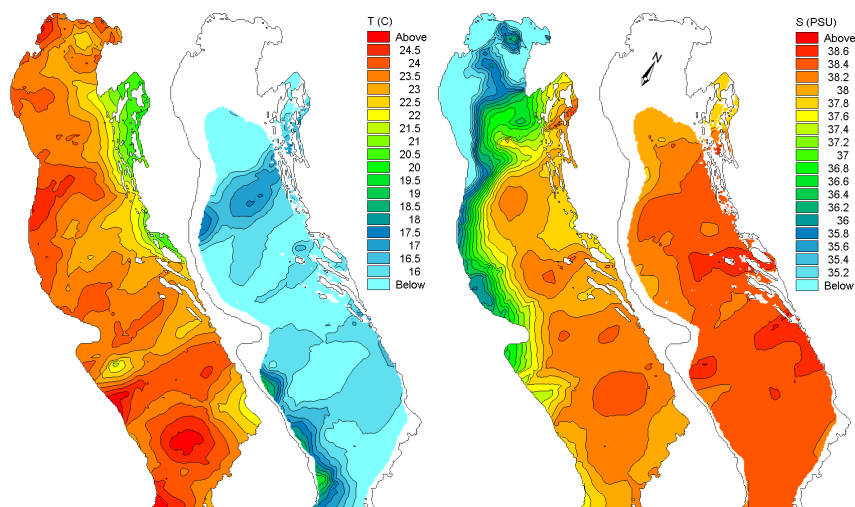

Figure 5 Sea temperature and salinity fields in the surface layer and at a depth of 50m for the area of the entire Adriatic (summer period - 1 July 2008 [25])

At the open boundaries the model was forced with hourly dynamic of sea levels [35], along with the sea temperature (T) and salinity (S) fields according to the measured vertical distributions of T and S at the nearest oceanographic station used within the implementation of this monitoring program JP-07/09 (Fig. 6).
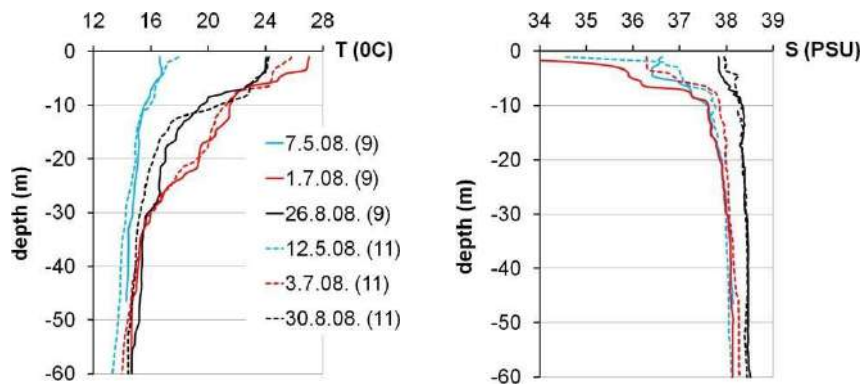
Figure 6 Measured vertical distributions of T and S at the oceanographic stations 8 and 11

Freshwater river inflows were defined with daily means for discharge and temperature, on the basis of measured data (Fig. 7). Salinity is parameterized with 0 PSU.

The fields of wind, air temperature, humidity and cloudiness were defined based on the results of the atmospheric numerical model Aladin-HR [36]-[40]. The used wind fields from the model Aladin-HR have a forecasting character (+12h) and spatial and temporal resolution of 8km and 3h, respectively (Figure 8).
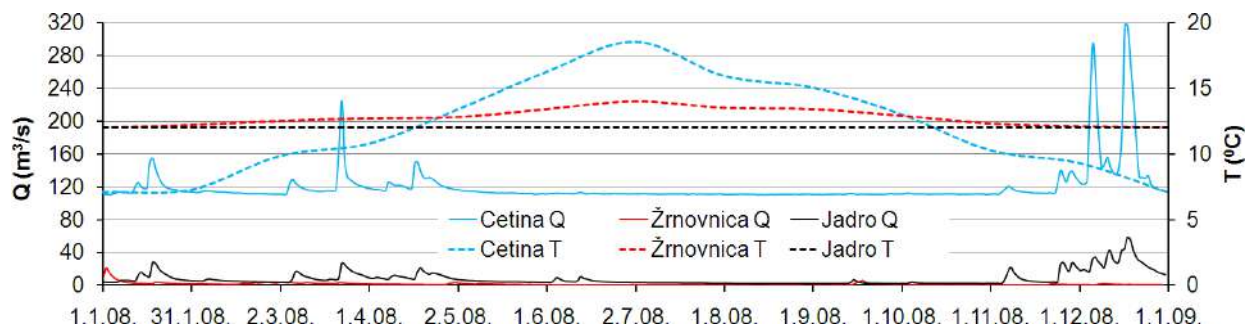
Figure 7 Time series of measured river discharges and temperature
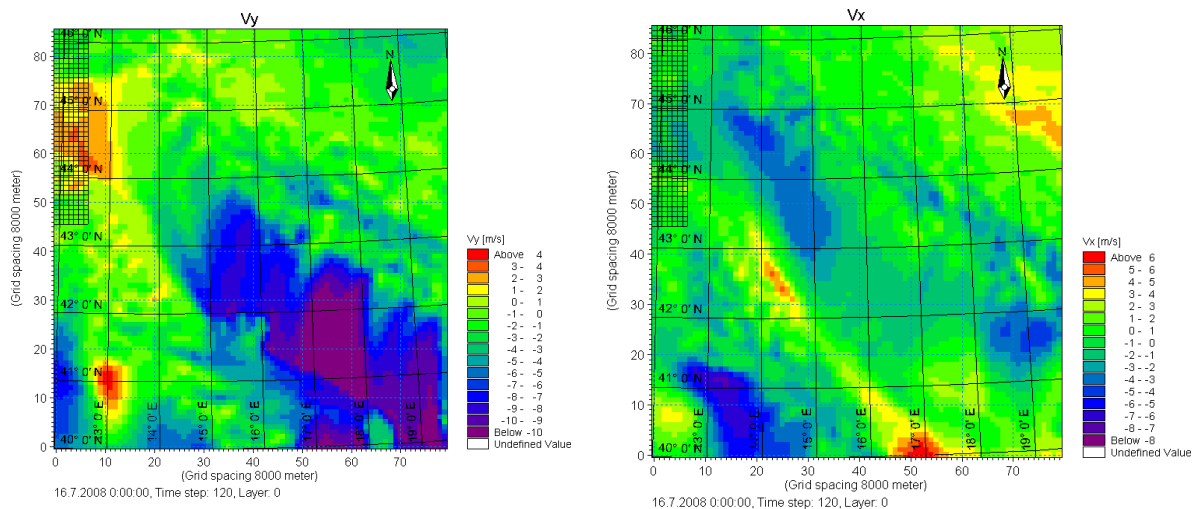
Figure 8 Example of resultant fields from the atmospheric model Aladin-HR for the term 16/7/08 0:00 (left - v_x wind velocity component at 10m from the sea surface; right - v_y velocity component))

2.3. Far field transport model for E.Colli

The user designs mathematical form to interpret time dynamics of E.Colli concentration within ecological processes with all interactions and connections among variables in a process. Defined process variables are spatially transferred through the connection with a convective dispersive module or hydrodynamic module.

Every designed mathematical form uses process variables, constants, forcing parameters and auxiliary variables, all incorporated through process equations. Process variables give the best insight into a state of a particular eco system and are chosen to predict system behavior by monitoring of their dynamics. Constants are used as arguments in mathematical formulas describing systems, and are time invariant but can be spatial variables. Forcing parameters are used as arguments in mathematical formulas describing systems, and can be both spatial and time variables. These parameters represent variables by which external influences on eco system e.g. temperature, solar radiation, wind etc., are involved. Auxiliary variables are also arguments in mathematical (numerical) formulas describing systems, and are sometimes used for direct result specification only. Processes give a mathematical description of the process variable transformation, meaning that processes are used as arguments in differential equations which are solved by ecological module for determination of the state of a process variable.

An ordinary differential equation is specified for each state variable. The ordinary differential equation summaries the processes evolved for the specific state variable. If a process affects more than one state variable, or the state variables affect each other, the differential equations are coupled with each other. The state variables are coupled linearly or non-linearly to each other through the source/sink terms. Defined numerical equations are solved using the built-in solver that makes an explicit time-integration of the transport equations when calculating the concentrations to the next time step. An approximate solution is obtained by treating the advection-dispersion term as constant in each time step. Defined coupled set of ordinary differential equations are solved by integrating the rate of change due to both the defined processes themselves and the advection-dispersion processes.

In E.Coli transport analysis the numeric formulation which treats E.Colli concentration as process variables of the ecosystem is used. The differential equation of the rate of E.Colli concentration change is created, using appropriate variables, constants, forcing parameters and auxiliary variables. Decay of E.Colli is described by the linear model of decay (Lee, 2011 [41]):

$$\frac{dC}{dt} = -[K * STI * C] \qquad ; \qquad K = \frac{Ln(10)}{T_{90}} \qquad \qquad (13)$$

where: C E.Colli concentration [1/100ml], K decay coefficient at 20°C in fresh water in darkness (1,08 1/dan, De Brauwere et al. [42]), STI correction decay coefficient for temperature, salinity, and light,

$$STI = \theta_T^{T-20} * \theta_S^S * \theta_I^{I(t,z)} \tag{14}$$

where: θ_T temperature correction coefficient for decay coefficient at temperatures different from 20 C^0 (1,09 – Jorgensen, 2001 [43]), T sea temperature, θ_S correction coefficient for salinity different from clean water (1,006 - Jorgensen, 2001), S salinity, θ_I correction coefficient for the influence of light (7,4 - Jorgensen, 2001 [43]).

A2/1

Vertical light distribution is defined by exponential law as a function of depth according to the Lambert-Beer law:

$$I(t,z) = f(t) \, I_0 \, e^{-kz} \tag{15}$$

where: I_0 light intensity at the surface at noon ($k = 2,3$/secchi depth).

3. COMBINIG MEASUREMENTS AND MODELS

Model simulations for sea circulation are performed for the period 10 May 2008 - 25 August 2008, since monitoring was conducted in that period on enough number of current meter and CTD measuring stations, which resulted in extensive set of data suitable for the verification of model results of thermohaline properties and sea circulation.

Comparison of measured and modelled vertical profiles of sea temperature and salinity is shown in figure 9.

Comparison of modelled and measured hourly averaged circulation velocities (u and v components) is given in the form of graphical interpretation for the position of oceanographic stations S13 and S14 (Figs. 10 and 11).

Presentation of averaged model current fields for the period from 10/5 to 1/7/2008, for depths of -2m, -20m and -40m is given in Figure 12.

Model maximum E.Colli concentration fields at the depths of -2m, -10m, -20m, -30 and -40m for the whole simulation period 10.5. – 25.8.08. are shown in Figure 13.
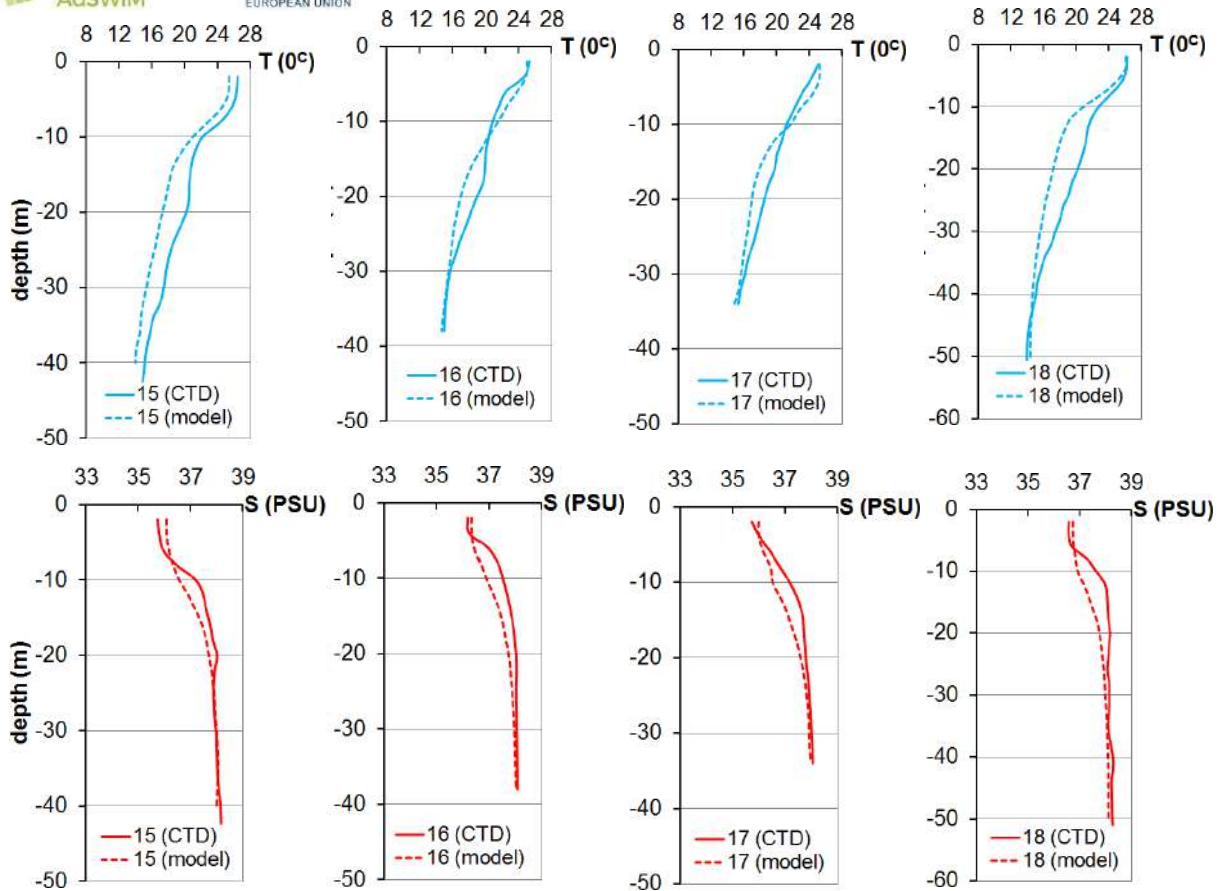
Figure 9 Comparison of measured and modelled vertical profiles of sea temperature (above) and sea salinity (below) for oceanographic stations 15, 16, 17 and 18 on 1 July 2008
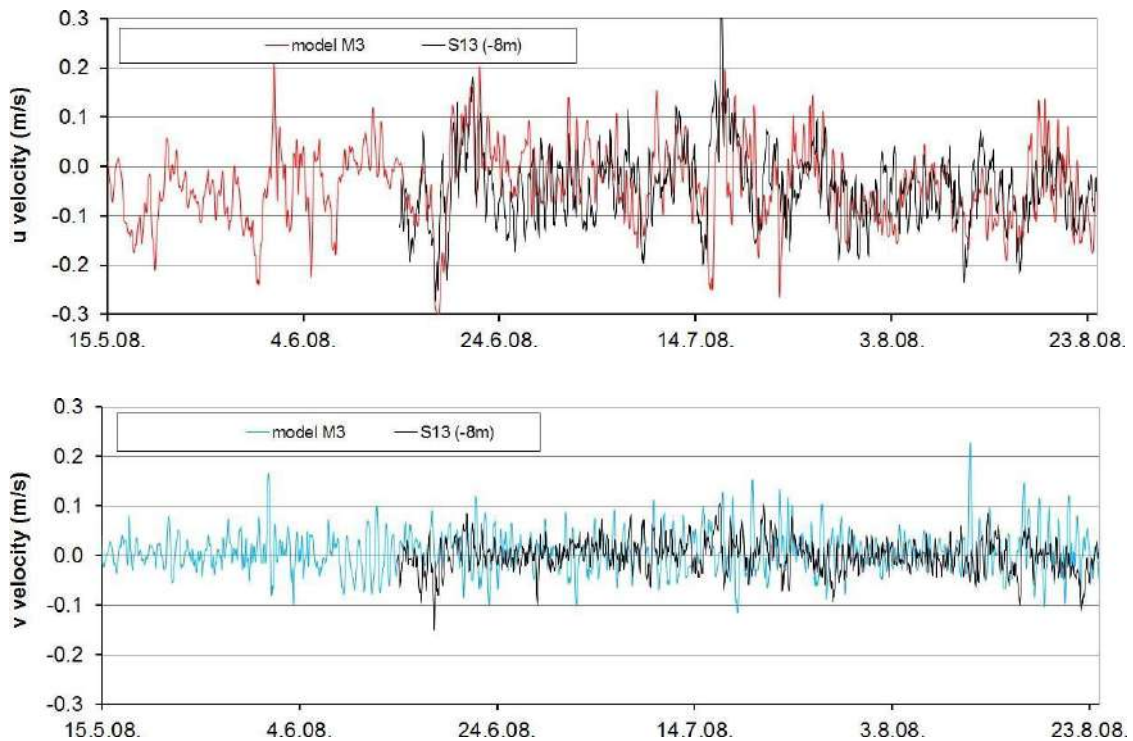

Figure 10a Comparison of measured (black) and modelled velocity components for position of station S13 at 8m depth
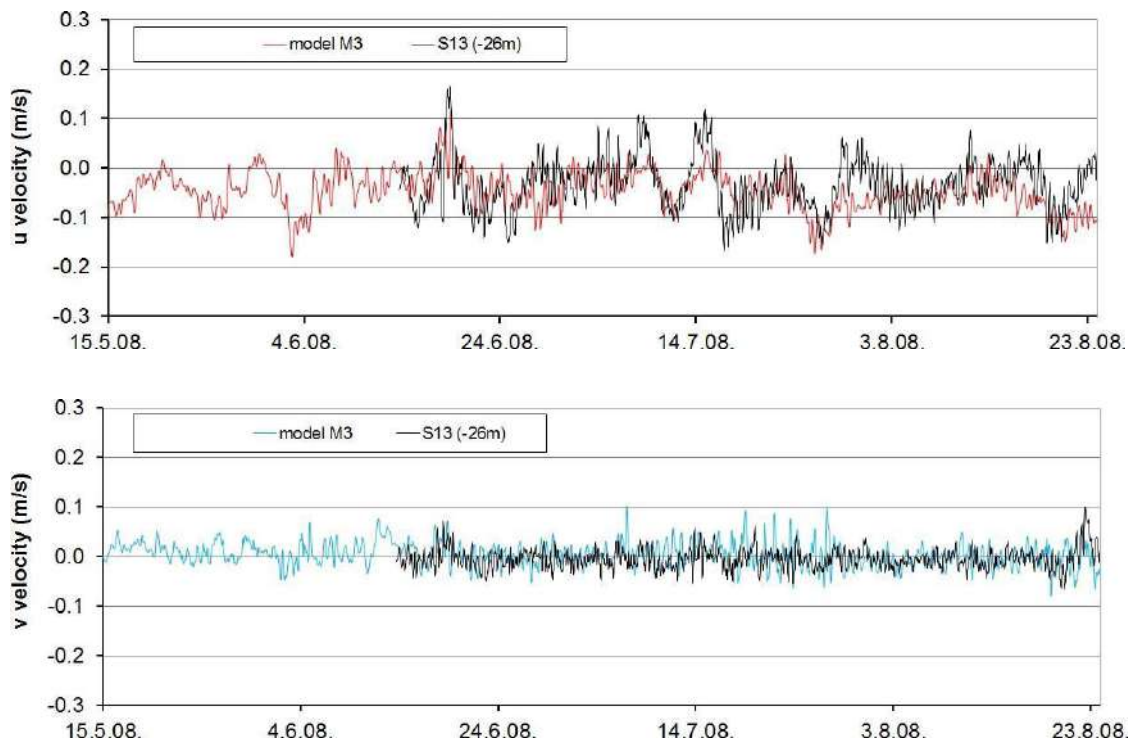
Figure 10b Comparison of measured (black) and modelled velocity components for position of station S13 at 26m depth
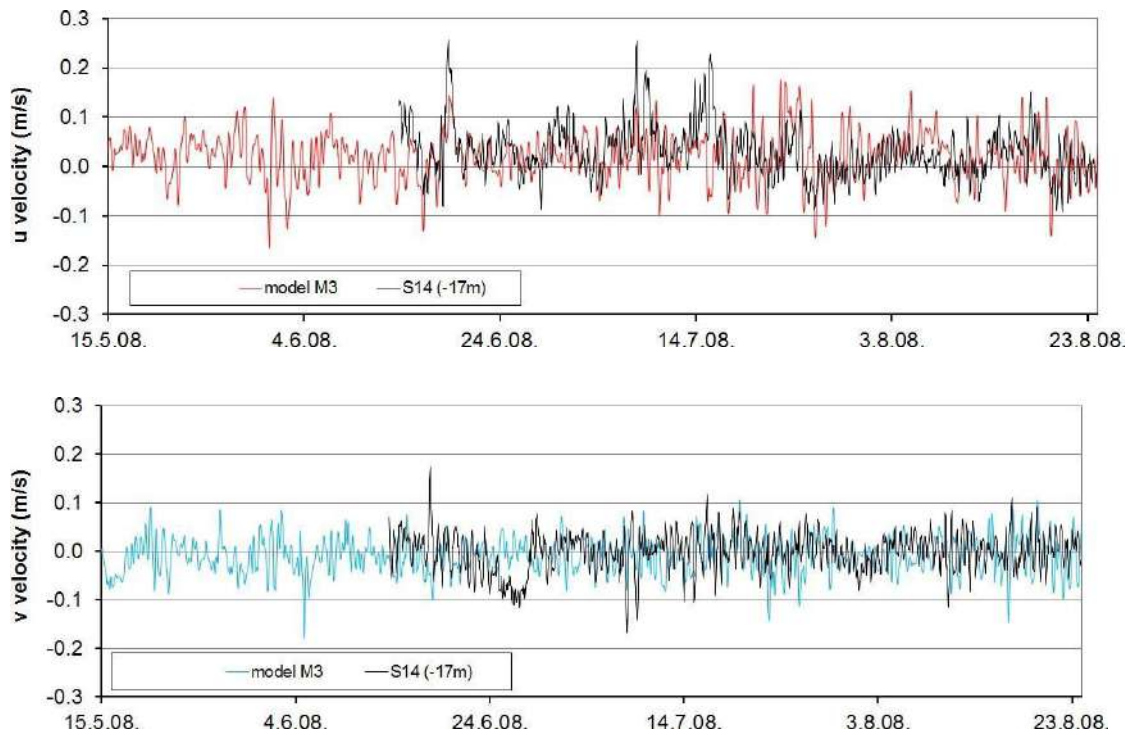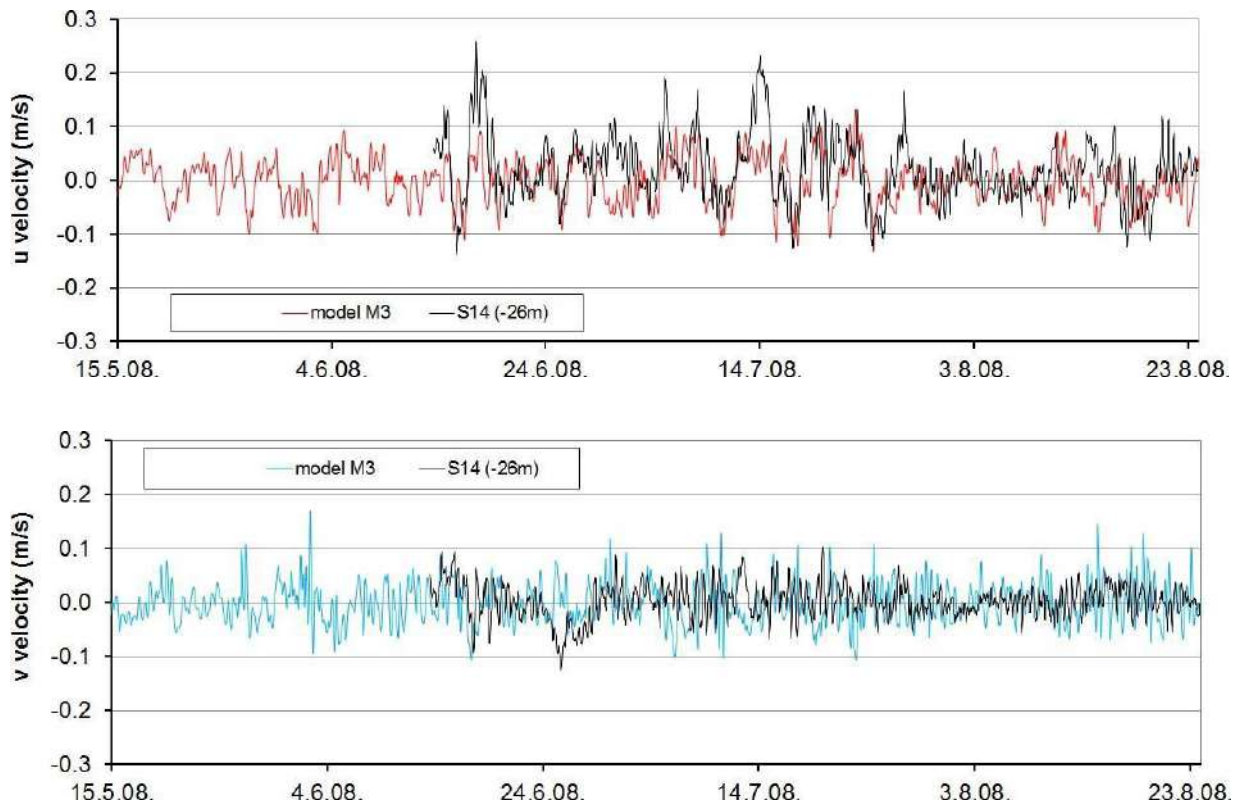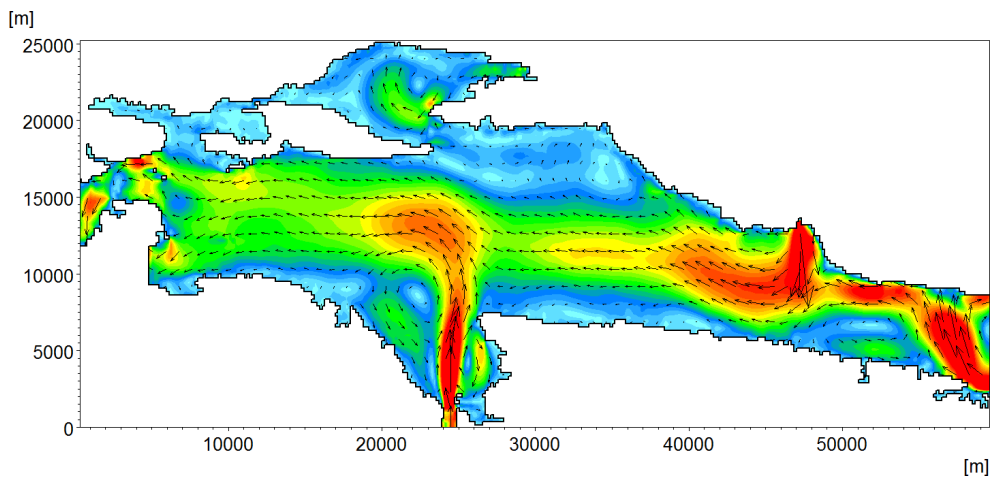

Figure 11a Comparison of measured (black) and modelled velocity components for position of station S14 at 17m depth

Figure 11b Comparison of measured (black) and modelled velocity components for position of station S14 at 26m depth
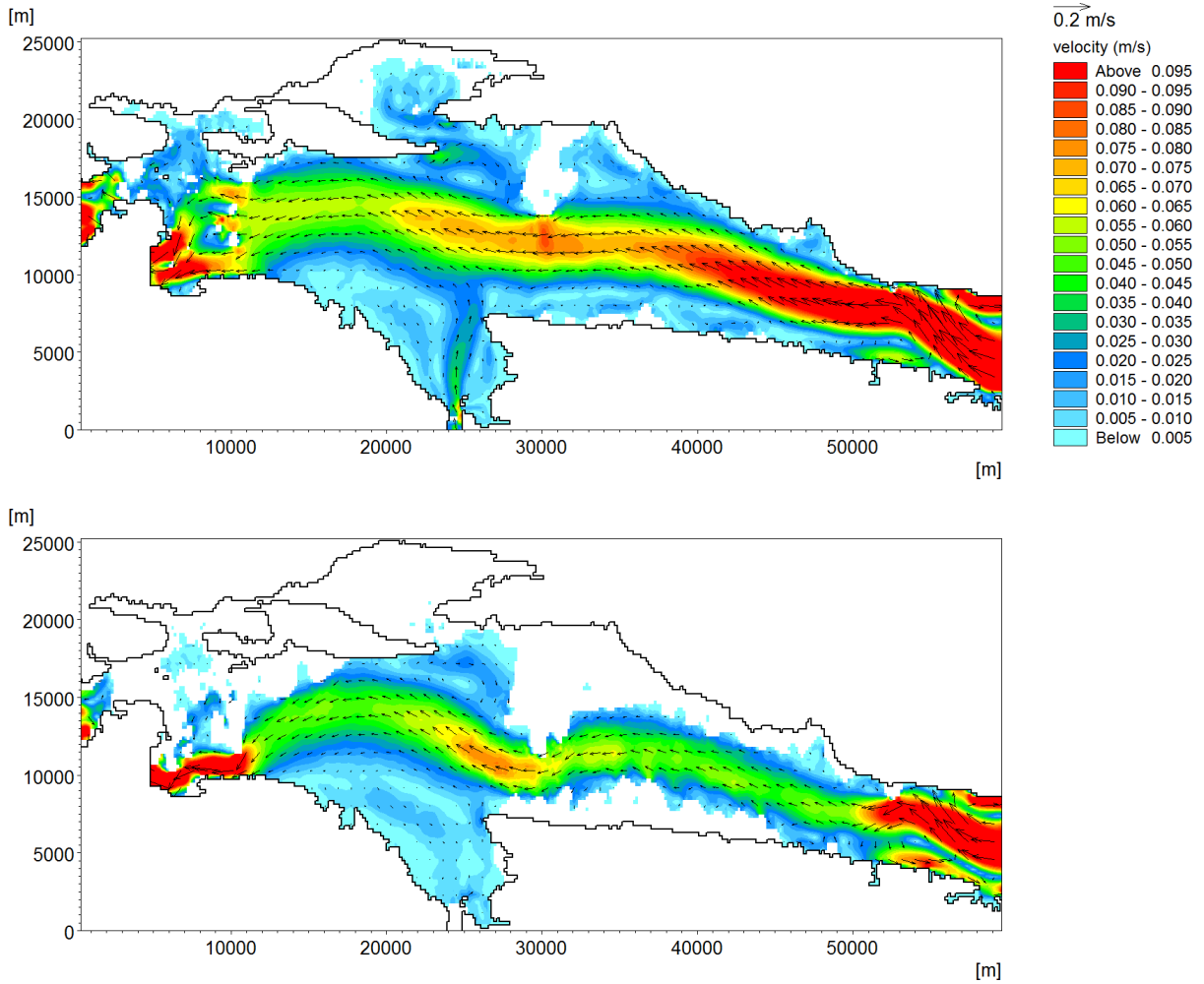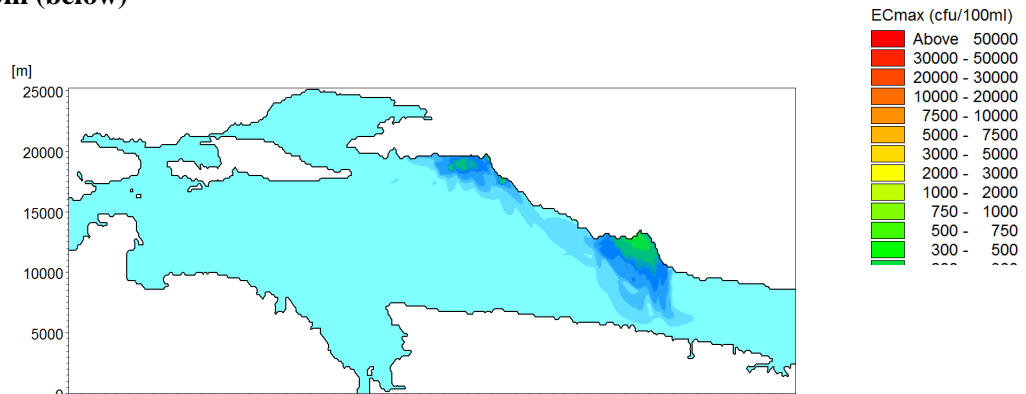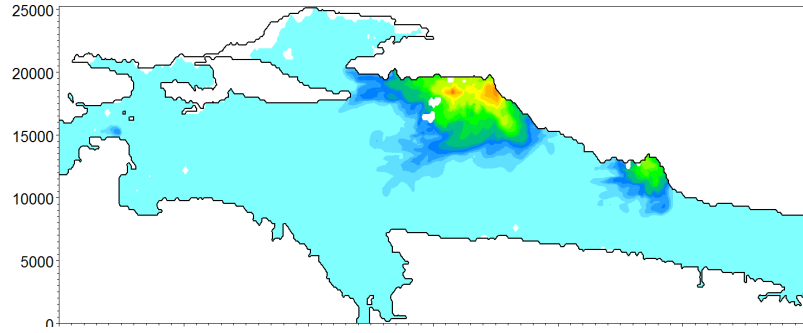
Figure 12 Averaged model current field for period 10.5.-1.7.2008. at a depth of -2m (above), -20m (middle) and -40m (below)
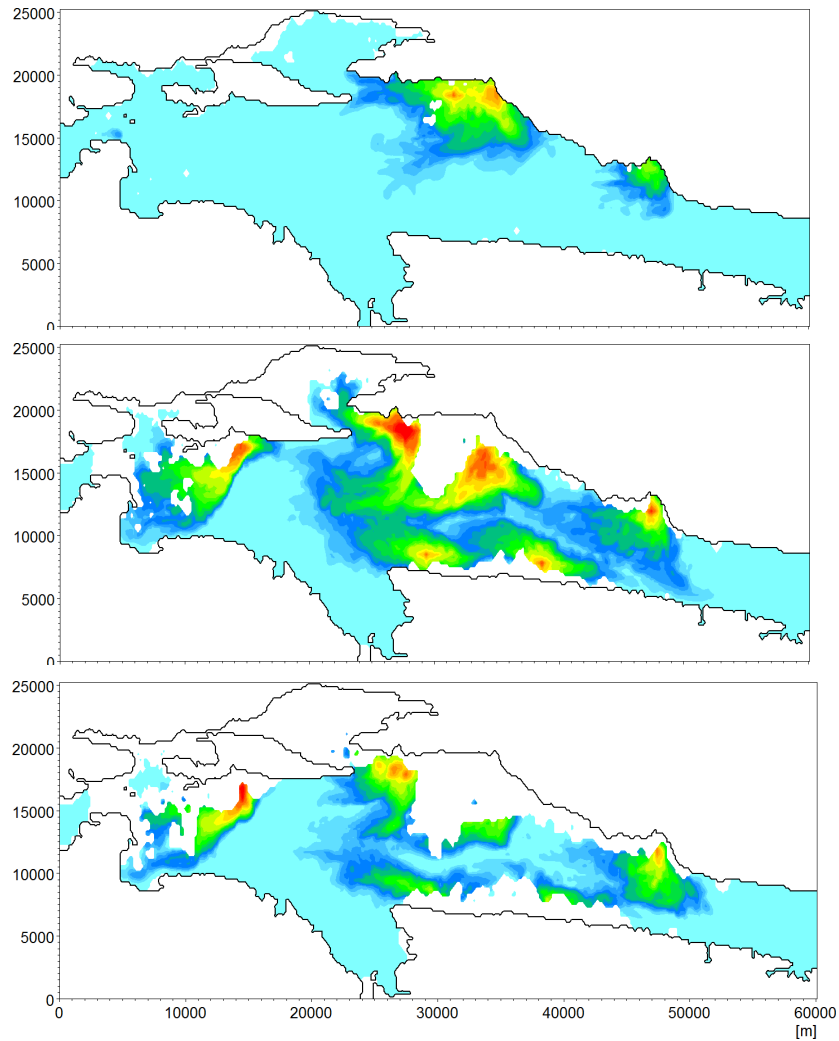
Figure 13 Model maximum E.Colli concentration fields at the depths of -2m, -10m, -20m, -30m and -40m for the whole simulation period 10.5.08 – 25.8.08.

REFERENCES

[1] R. Sterneck, "Zur hydrodynamischen Teorie der Adriagezeiten", *Sitzungsberichte der Kaiserlichen Akademie der Wissenschaften in Wien*, Vol. 124, 1915, pp. 147-180

[2] R. Sterneck, "Gezeitenerscheinungen der Adria - II. Teil. Die theoretische Erklärung der Beobachtungstatsachen", *Denkschriften der Akademie der Wissenschaften in Wien*, Vol. 96, 1919, pp. 277-324

[3] A. Defant, *Annalen der Hydrographie und Maritimen Meteorologie*, Vol. 48, 1920, pp. 163- 169

[4] E. Accerboni, B. Manca, "Storm surges forecasting in the Adriatic Sea by means of a two- dimensional hydrodynamical numerical model", *Boll. Geofis Teor. Appl.*, Vol. XV, 1973, pp. 3-22

[5] F. Stravisi, "A numerical experiment on wind effects in the Adriatic Sea", *Accademia Nazionale dei Lincei, Rendiconti della Classe di Scienze Fisiche, Matematiche e Naturali*, Ser. VIII, Vol. LII, 1972, pp. 187-196

[6] F. Stravisi, "Analysis of a storm surge in the Adriatic Sea by means of a two-dimensional linear model", *Accademia Nazionale dei Lincei, Rendiconti della Classe di Scienze Fisiche, Matematiche e Naturali*, Ser. VIII, Vol. LIV, 1973, pp. 243-260

[7] C. Finizio, S. Palmieri, A. Riccucci, "A numerical model of the Adriatic for the prediction of high tides at Venice" *Met. Soc.*, Vol. 98, 1972, pp. 86-104

[8] A.R. Robinson, A. Tomasin, A. Artegiani, "Flooding of Venice: Phenomenology and prediction of the Adriatic storm surge", *Met. Soc.*, Vol. 99, 1973, pp. 688-692

[9] M. Kuzmić, M. Orlić, M. Karabeg, Lj. Jeftić, "An investigation of wind-driven topographically controlled motions in the Northern Adriatic", *Estuar. Coastal Shelf Sci.*, Vol. 21, 1985, pp. 481-499

[10] M.C. Hendershott, P. Rizzoli, "The winter circulation of the Adriatic Sea", *Deep-Sea Res.*, Vol. 23, 1976, pp. 353-370

[11] M. Kuzmić, M. Orlić, "Wind induced vertical shearing - Alpex/Medalpex data and modelling excercise", *Annales Geophysicae B*, Vol. 5, 1987, pp. 103-112

[12] M. Bone, "On topographic and wind vorticity effects in bora driven circulation in the North Adriatic", *Geofizika*, Vol. 4, 1987, pp. 129-135

[13] M. Orlić, M. Kuzmić, Z. Pasarić, "Response of the Adriatic Sea to the bora and sirocco forcing", *Cont. Shelf Res.*, Vol. 14, 1994, pp. 91-116

[14] D.C.Jr. Gordon, P.R. Boudreau, K.H. Mann, J.E. Ong, W.L. Silvert, S.V. Smith, G. Wattayakorn, F. Wulff, T. Yanagi, "Biogeochemical modelling guidelines", *LOICZ*, Vol. 5, 1995, Texel, The Netherlands, pp. 96

[15] E. Hofmann, C. Lascara, "Overview of Interdisciplinary Modeling for Marine Ecosystems", In: K.H. Brink, A.R. Robinson (Eds.), *The Sea*, Vol. 10, 1998, pp. 507-540

[16] J. McCarthy, A. Robinson, B. Rothschild, "Biological - physical interactions in the sea: emergent findings and new directions", In: A. Robinson, J. McCarthy, B. Rothschild (Eds.), *The Sea*, Vol. 12, 2002, pp. 1-17

[17] K.L. Denman, "Modelling planktonic ecosystems: parameterizing complexity", *Prog. Oceanogr.*, Vol. 57, 2003, pp. 429-452

[18] J. Baretta, W. Ebenhöh, P. Ruardij, "The European Regional Seas Ecosystem Model, a complex marine ecosystem model", *J. Sea Res.*, Vol. 33, 1995, pp. 233-246

[19] J. Baretta-Bekker, J. Baretta, W. Ebenhoeh, "Microbial dynamics in the marine ecosystem model ERSEM II with decoupled carbon assimilation and nutrient uptake", *J. Sea Res.*, Vol. 38, 1997, pp. 195-212

[20] M. Vichi, M. Zavatarelli, N. Pinardi, "Seasonal modulation of microbial - mediated carbon fluxes in the Northern Adriatic Sea", *Fisheries Oceanogr.*, Vol. 7, 1998, pp. 182-190

[21] M. Zavatarelli, J. Baretta, J. Baretta-Bekker, N. Pinardi, "The dynamics of the Adriatic Sea ecosystem; an idealized model study", *Deep-Sea Res.*, Vol. 47, 2000, pp. 937-970

[22] M. Vichi, P. Ruardij, J.W. Baretta, "Link or sink: a modelling interpretation of the open Baltic biogeochemistry", *Biogeosciences*, Vol. 1, 2004, pp. 79-100

[23] C. Raick, E.J.M. Delhez, K. Soetaert, M. Gregoire, "Study of the seasonal cycle of the biogeochemical processes in the Ligurian Sea using a ID interdisciplinary model", *J. Mar. Syst.*, Vol. 55, 2005, pp. 177-203

[24] M. Vichi, W. May, A. Navarra, "Response of a complex ecosystem model of the northern Adriatic Sea to a

regional climate change scenario", *Clim. Res.*, Vol. 24, 2003, pp. 141-159

[25] Fischer, H.B., List, E.J., Koh, R., Imberger, J., Brooks, N.H. (1979.): *Mixing in Inland and Coastal Waters*, Academic Press, 1979.

[26] Cushman-Roisin, B., Gualtieri, C., Mihailović, D.T., 2008, *Environmental fluid mechanics: Current issues and future outlook, In: Fluid Mechanics of Environmental Interfaces* (C. Gualtieri and D.T. Mihailović Eds.), Taylor & Francis, 2008, 1-13.

[27] Akar, P. J., Jirka, G. H. (1994): Buoyant Spreading Processes in Pollutant Transport and Mixing, Part 1: Lateral spreading with ambient current advection, *Journal of Hydraulic Research*, 32(6), 427-439.

[28] Akar, P. J., Jirka, G. H. (1994): Buoyant Spreading Processes in Pollutant Transport and Mixing, Part 2: Upstream spreading in weak ambient current, *Journal of Hydraulic Research*, 33(1), 24-37.

[29] Wood, I.R., Bell, R.G., Wilkinson, D. L., 1993, *Ocean Disposal of Wastewater*, Advanced Series on Ocean Engineering – Volume 8, World Scientific, London. 425 pp.

[30] Pun, K.L., Davidson, M. J., 1999, *On the behaviour of advected plumes and thermals*, Journal of Hydraulic Research, 37(4), 296-311.

[31] Featherstone, R.E. (1984): Mathematical models of the discharge of wastewater into a marine environment, *In: James, A. (Ed.), An Introductory to Water Quality Modelling*, first ed. Wiley, Chichester, 150–162.

[32] Turner, J.S. (1986): Turbulent entrainment: the development of the entrainment assumption, and its application to geophysical flows, *J. Fluid Mech.*, 173, 431–471.

[33] Fan, L.N., Brooks, N.H. (1966): Horizontal jets in stagnant fluid of other density, *J. Hydraul. Divn.*, ASCE 92, 423–429.

[34] C. Galos, *Seasonal circulation in the Adriatic Sea*, M.S. thesis, Dartmouth Coll., Hanover, 2000.

[35] I. Janeković, M. Kuzmić, "Numerical simulation of the Adriatic Sea principal tidal constituents", *Ann. Geophys.*, Vol. 23, 2005, pp. 3207–3218

[36] P.C. Courtier, J.F. Freydier, F. Geleyn, M. Rochas, "The ARPEGE project at METEO- FRANCE", *Proceedings from the ECMWF workshop on numerical methods in atmospheric models*, Vol. 2, Reading, England, 1991, pp. 193-231

[37] E. Cordoneanu, J.F. Geleyn, "Application to local circulation above the Carpathian-Black Sea area of a NWP-type meso-scale model", *Contributions to Atmospheric Physics*, Vol. 71, 1998, pp. 191-212

[38] N. Brzović, "Factors affecting the Adriatic cyclone and associated windstorms", *Contributions to Atmospheric Physics*, Vol. 72, 1999, pp. 51-65

[39] N. Brzović, N. Strelec-Mahović, "Cyclonic activity and severe jugo in the Adriatic", *Physics and Chemistry of the Earth (B)*, Vol. 24, 1999, pp. 653-657

[40] S. Ivatek-Sahdan, M. Tudor, "Use of high-resolution dynamical adaptation in operational suite and research impact studies", *Meteorol. Z.*, Vol. 13, 2004, pp. 99-108.

[41] Lee, C.W. Yee, A., Fang Ng, Bong, C.W., Narayanan, K., Sim, E.U.H., Ng, C.C. (2011): Investigating the decay rates of Escherichia coli relative to Vibrio parahemolyticus and Salmonella Typhi in tropical coastal waters, *Water Research*, 45(4), pp. 1561-1570.

[42] De Brauwere, A., De Brye, B., Servais, P., Passerat, J., Deleersnijder, E. (2011.): Modelling Escherichia coli concentrations in the tidal Scheldt river and estuary. *Water Res.* , 45, 2724–2738.

[43] Jorgensen, S., Bendoricchio, G. (2001.): *Fundamentals of ecological modelling*, Elsevier- academic press, 2001.